

# Journal of Molecular Structure

## Three isomeric 4-[(n-bromophenyl)carbamoyl]butanoic acids (n = 2, 3, and 4) as DNA intercalator: Synthesis, physiochemical characterization, antimicrobial activity, antioxidant potential and in silico study

--Manuscript Draft--

<b>Manuscript Number:</b>	MOLSTRUC-D-21-05517
<b>Article Type:</b>	Research Paper
<b>Keywords:</b>	4-[(n-bromophenyl) carbamoyl]butanoic acids; X-ray crystallography; DNA intercalator; antimicrobial activity; DPPH scavenging; in silico study
<b>Corresponding Author:</b>	Dr. Muhammad Siraj Sirajuddin, Ph.D University of Science & Technology, Bannu, Pakistan Bannu, PAKISTAN
<b>First Author:</b>	Bibi Hanifa, PhD
<b>Order of Authors:</b>	Bibi Hanifa, PhD Dr. Muhammad Siraj Sirajuddin, Ph.D Maciej Kubicki, Postdoc Edward R. T. Tiekink, Postdoc
<b>Abstract:</b>	A series of three isomeric 4-[(n-bromophenyl)carbamoyl]butanoic acids (n = 2, 3, and 4) were synthesized and their structures confirmed by FTIR, NMR, MS, micro elemental analysis (CHN) and single crystal X-ray crystallography. Kinks are noted in the molecular structures of the n = 2 and n = 3 compounds, namely about the methylene-C-C(carbonyl) and N-C(phenyl) bonds; no such twist about the former bond is seen in the n = 4 molecule. In the molecular packing, supramolecular tapes are evident, being constructed by orthogonally orientated carboxylic acid-O-H...O(carbonyl) and amide-N-H...O(amide) hydrogen bonds. The compounds were evaluated for interaction with salmon sperm DNA and found that they bind via an intercalative mode resulting in hypochromism and bathochromic shift as confirmed by the UV-visible spectroscopic and viscometric techniques. The results of antimicrobial activity performed against five bacterial and two fungal strains show that these compounds have < 50% inhibition. The DPPH antioxidant activity results revealed 78% maximum scavenging activity. An in silico study performed using the SwissADME webserver revealed the compounds obey the rules of drug-likeness and exhibit good potential for bioavailability.
<b>Suggested Reviewers:</b>	Muhammad Tariq, PhD Professor, BZU: Bahauddin Zakariya University mtnazir@yahoo.com  Hameed Ullah, postdoc Professor, Islamia College Peshawar hameedwazir@yahoo.co.uk  Muhammad Iqbal, PhD Professor, Bacha Khan University Charsadda iqbalmo@yahoo.com

Dear Editor,

I am submitting a manuscript entitled **“Three isomeric 4-[(n-bromophenyl)carbamoyl]butanoic acids (n = 2, 3, and 4) as DNA intercalator: Synthesis, physicochemical characterization, antimicrobial activity, antioxidant potential, and *in silico* study”** by Bibi Hanifa, Muhammad Sirajuddin, Maciej Kubicki, Edward R. T. Tiekink for possible publication in Journal of Molecular Structure. The art of this paper is in accordance to the standard format of this journal and contains a complete set of informations for the readers working in the fields of chemistry.

A series of three isomeric 4-[(n-bromophenyl)carbamoyl]butanoic acids (n = 2, 3, and 4) were synthesized and their structures confirmed by FTIR, NMR, MS, micro elemental analysis (CHN) and single crystal X-ray crystallography. Kinks are noted in the molecular structures of the n = 2 and n = 3 compounds, namely about the methylene-C–C(carbonyl) and N–C(phenyl) bonds; no such twist about the former bond is seen in the n = 4 molecule. In the molecular packing, supramolecular tapes are evident, being constructed by orthogonally orientated carboxylic acid-O-H...O(carbonyl) and amide-N-H...O(amide) hydrogen bonds. The compounds were evaluated for interaction with salmon sperm DNA and found that they bind *via* an intercalative mode resulting in hypochromism and bathochromic shift as confirmed by the UV-visible spectroscopic and viscometric techniques. The results of antimicrobial activity performed against five bacterial and two fungal strains show that these compounds have < 50% inhibition. The DPPH antioxidant activity results revealed 78% maximum scavenging activity. An *in silico* study performed using the SwissADME webserver revealed the compounds obey the rules of drug-likeness and exhibit good potential for bioavailability.

The manuscript has neither been previously published, nor submitted to any other journal. I trust that this manuscript will prove acceptable for publication.

Yours sincerely,

M. Sirajuddin

## Highlights

- Synthesis of three isomeric 4-[(n-bromophenyl)carbamoyl]butanoic acids
- Structural and spectroscopic characterization
- Interaction with SSDNA *via* intercalative mode of interaction
- Antioxidant and antimicrobial activities
- *In silico* study

1  
2  
3  
4 **Three isomeric 4-[(n-bromophenyl)carbamoyl]butanoic acids (n = 2, 3, and 4) as DNA**  
5 **intercalator: Synthesis, physicochemical characterization, antimicrobial activity, antioxidant**  
6 **potential and *in silico* study**  
7  
8

9 **Bibi Hanifa<sup>a</sup>, Muhammad Sirajuddin<sup>a,\*</sup>, Maciej Kubicki<sup>b</sup>, Edward R. T. Tiekink<sup>c</sup>**

10 <sup>a</sup>Department of Chemistry, University of Science and Technology Bannu 28100, Pakistan

11 <sup>b</sup>Department of Chemistry, Adam Mickiewicz University in Poznan, Poznan, 61-712, Poland

12 <sup>c</sup>Centre for Crystalline Materials, School of Medical and Life Sciences, Sunway University, No.  
13 5 Jalan Universiti, Bandar Sunway 47500, Selangor Darul Ehsan, Malaysia

14 \*Corresponding author address: [m.siraj09@gmail.com](mailto:m.siraj09@gmail.com) (M. Sirajuddin)

15  
16  
17  
18  
19  
20 **Abstract**

21  
22 A series of three isomeric 4-[(n-bromophenyl)carbamoyl]butanoic acids (n = 2, 3, and 4) were  
23 synthesized and their structures confirmed by FTIR, NMR, MS, micro elemental analysis (CHN)  
24 and single crystal X-ray crystallography. Kinks are noted in the molecular structures of the n = 2  
25 and n = 3 compounds, namely about the methylene-C–C(carbonyl) and N–C(phenyl) bonds; no  
26 such twist about the former bond is seen in the n = 4 molecule. In the molecular packing,  
27 supramolecular tapes are evident, being constructed by orthogonally orientated carboxylic acid-O-  
28 H...O(carbonyl) and amide-N-H...O(amide) hydrogen bonds. The compounds were evaluated for  
29 interaction with salmon sperm DNA and found that they bind *via* an intercalative mode resulting  
30 in hypochromism and bathochromic shift as confirmed by the UV-visible spectroscopic and  
31 viscometric techniques. The results of antimicrobial activity performed against five bacterial and  
32 two fungal strains show that these compounds have < 50% inhibition. The DPPH antioxidant  
33 activity results revealed 78% maximum scavenging activity. An *in silico* study performed using  
34 the SwissADME webserver revealed the compounds obey the rules of drug-likeness and exhibit  
35 good potential for bioavailability.  
36  
37  
38  
39  
40  
41  
42  
43  
44  
45  
46  
47

48 **Keywords:** 4-[(n-bromophenyl) carbamoyl]butanoic acids; X-ray crystallography; DNA  
49 intercalator; antimicrobial activity; DPPH scavenging; *in silico* study  
50  
51  
52  
53

54 **1. Introduction**

55 Carboxylic acid derivatives of amides play an important role in prodrug design due to their easy  
56 enzymatic hydrolysis [1] as well as feature as a valuable part of pharmacophores of diverse classes  
57 of therapeutic agents [2] despite the carboxylic functional group having several potential  
58  
59  
60  
61  
62  
63  
64  
65

1  
2  
3  
4 shortcomings such as metabolic instability, toxicity, as well as limited passive diffusion across  
5 biological membranes [3]. It is estimated about > 450 drugs contain carboxylic acid functional  
6 groups which are marketed Worldwide, e.g., nonsteroidal anti-inflammatory drugs (NSAIDs) such  
7 as naproxen, ibuprofen, indomethacin, cetylsalicylic acid (aspirin), salicylic acid, diclofenac,  
8 mefenamic acid, flufenamic acid, etc., antibiotics such as cephalosporin antibiotics (e.g.,  
9 cephalothin, cephacetrile, cephapirin, cephaloridine, etc.) and penicillin antibiotics (e.g.,  
10 benzylpenicillin, phenethicillin, methicillin, nafcillin, etc.), quinolone antibiotics (e.g.,  
11 ciprofloxacin, norfloxacin, acrosoxacin, piperidic acid, nalidixic acid, etc.), anticoagulants (e.g.,  
12 heparin), cholesterol-lowering statins (e.g., omega-3 carboxylic acids), among others [3]. The  
13 importance of these compounds relates to favorable drug-target interaction owing to their acidity  
14 and ability to form a strong electrostatic as well as hydrogen bonding interactions [4, 5].

15  
16  
17  
18  
19  
20  
21  
22  
23  
24 Due to the flexible binding nature of carboxylic acids, they form various supramolecular  
25 structures [6]. As a ligand, the carboxylate moiety plays an important role in the formation of  
26 coordination and organometallic compounds, often with desirable properties [7]. The carboxylate  
27 moiety can bind to metal in complexation either in ionic or covalent modes. In the later  
28 circumstances, coordination may be in monodentate, bridging or bidentate (which may be either  
29 *syn-syn* or *syn-anti*) modes [8].

30  
31  
32  
33  
34  
35 In the present study, glutaric acid-amide based carboxylic derivatives have been synthesized  
36 in order to generate compounds with enhanced solubility and bioavailability. Relatively limited  
37 literature is available for this class of compound. Thus, in 1973, Skinner and Sargent reported the  
38 syntheses of the *N*-(substituted)glutaramic acids by the condensation of equimolar amounts of the  
39 substituted amine and glutaric anhydride at 100°C for 3 h under anhydrous conditions; supporting  
40 spectroscopic and crystallographic data of these synthesized compounds were not provided. The  
41 original application for these compounds was as plant growth regulators [9]. Herein, an easy and  
42 economical method for the synthesis of glutaric anhydride based carboxylic derivatives is  
43 described requiring only room temperature conditions and with a maximum of 3-5 min reaction  
44 time.

45  
46  
47  
48  
49  
50  
51  
52  
53 Small organic molecules can bind to DNA either in covalent or non-covalent mode resulting  
54 the alteration or inhibition of DNA function. Those molecules which bind to nitrogenous bases of  
55 DNA lead to the inhibition of cell division through interference with DNA replication and  
56 transcription processes. Another possible mechanism for their anticancer activity is that  
57  
58  
59  
60  
61  
62  
63  
64  
65

1  
2  
3  
4 proliferation of the cells is halted by affecting the multienzyme complexes with are responsible for  
5 the DNA replication and transcription [1, 10-11].  
6

7  
8 Keeping in view the importance of these compounds as well as in continuation of previous  
9 research in this area, in this article are reported the synthesis, characterization and biological  
10 evaluation, namely DNA binding, antimicrobial and antioxidant potentials, of three isomeric 4-  
11 [(n-bromophenyl)carbamoyl]butanoic acids (n = 2, 3, and 4) compounds. The compositions of the  
12 synthesized compounds are confirmed by FTIR, NMR, MS, elemental analysis and X-ray  
13 crystallography. An *in silico* study of these compounds relating to their biological potential was  
14 also performed.  
15  
16  
17  
18  
19  
20  
21

## 22 **2. Materials and Methods**

23  
24 The substituted anilines (2-, 3-, and 4-bromoaniline) and glutaric anhydride were purchased from  
25 Macklin (Shanghai, China) and solvents were obtained Sigma (Saint Louis, MO, USA) and used  
26 without further purification. The melting points were determined on a BioCote melting point  
27 apparatus (Staffordshire, UK). Elemental analyses were performed on a PerkinElmer CHNS 2400  
28 instrument (Waltham, MA, USA). The FTIR spectra were measured on a Thermo Nicolet-6700  
29 spectrophotometer (Vienna, Austria) from 4000 to 450 cm<sup>-1</sup>. The <sup>1</sup>H and <sup>13</sup>C NMR spectra were  
30 recorded in DMSO-d<sub>6</sub> solution on a Bruker Avance 500-MHz NMR (Billerica, MA, USA)  
31 spectrometer. The DNA binding experiments were performed using a UH-5300 UV/Vis.  
32 spectrophotometer (Hitachi High Tech Science Corporation, Kyoto, Japan) and PSL ASTM  
33 Ubbelohde viscometer (Model: 65922, Essex, UK). The GC-MS spectrum was obtained using a  
34 Thermo Scientific TRACE™ 1310 Gas Chromatograph and Thermo Scientific ISQ™ Series  
35 Quadrupole GC-MS (Waltham, MA, USA) with conditions: carrier gas: helium; column gas flow:  
36 1.2 mL/s; constant flow; injection mode: splitless injection; column: Agilent HP 5MS, (30 m x  
37 0.25 mm x 25 μm); inlet temp.: 270 °C; oven temperature program: 40 °C (1 min) at 10 °C/min to  
38 300 °C (7 min); transfer line temp.: 300 °C; solvent delay: 2.5 min; ionization energy: 70 eV; ion  
39 source temp.: 230 °C; mass range: 35–550 amu, scan rate: 3 scan/s; software: Xcalibur.  
40  
41  
42  
43  
44  
45  
46  
47  
48  
49  
50  
51  
52  
53

### 54 **2.1 X-ray crystallography**

55  
56  
57 Diffraction data were collected by the ω-scan technique, at room temperature for on a Rigaku  
58 SuperNova four-circle diffractometer with Atlas CCD detector, equipped with Nova microfocus  
59  
60  
61  
62  
63  
64  
65

1  
2  
3  
4 CuK $\alpha$  radiation source ( $\lambda = 1.54184 \text{ \AA}$ ) for **1** and **3**; for **2**, data were collected on a Rigaku/Oxford  
5  
6 Diffraction XtaLAB Synergy diffractometer (Dualflex, AtlasS2) also fitted with CuK $\alpha$  radiation.  
7  
8 The data were processed, including correcting for absorption effects with CrysAlis PRO [12]. The  
9  
10 structures were solved with SHELXT (**1** and **3**)/SHELXS (**2**) [13] and refined by the full-matrix  
11  
12 least-squares procedure on  $F^2$  by SHELXL-2018/3 [14]. For **1** and **3**, all non-hydrogen atoms were  
13  
14 refined anisotropically, hydrogen atoms were placed in idealized positions and refined as ‘riding  
15  
16 model’ with isotropic displacement parameters set at 1.2 (1.5 for hydroxyl groups) times  $U_{eq}$  of  
17  
18 appropriate carrier atoms. For **2**, the O- and N-bound atoms were located from a difference map  
19  
20 and refined with but, were refined with O–H =  $0.82 \pm 0.01$  and N–H =  $0.86 \pm 0.01 \text{ \AA}$  distance  
21  
22 restraints, and with  $U_{iso}(H)$  set to  $1.5U_{equiv}(O)$  and  $1.2U_{equiv}(N)$ , respectively. A weighting scheme  
23  
24 of the form  $w = 1/[\sigma^2(F_o^2) + (aP)^2 + bP]$  where  $P = (F_o^2 + 2F_c^2)/3$  was introduced in each  
25  
26 refinement. The programs ORTEP-3 for Windows [15], PLATON [16], and DIAMOND [17] were  
27  
28 also used in the study. Crystal data and refinement details are given in Table 1.  
29  
30  
31  
32  
33  
34  
35  
36  
37  
38  
39  
40  
41  
42  
43  
44  
45  
46  
47  
48  
49  
50  
51  
52  
53  
54  
55  
56  
57  
58  
59  
60  
61  
62  
63  
64  
65

**Table 1**

Crystal data, data collection, and details of structure refinement

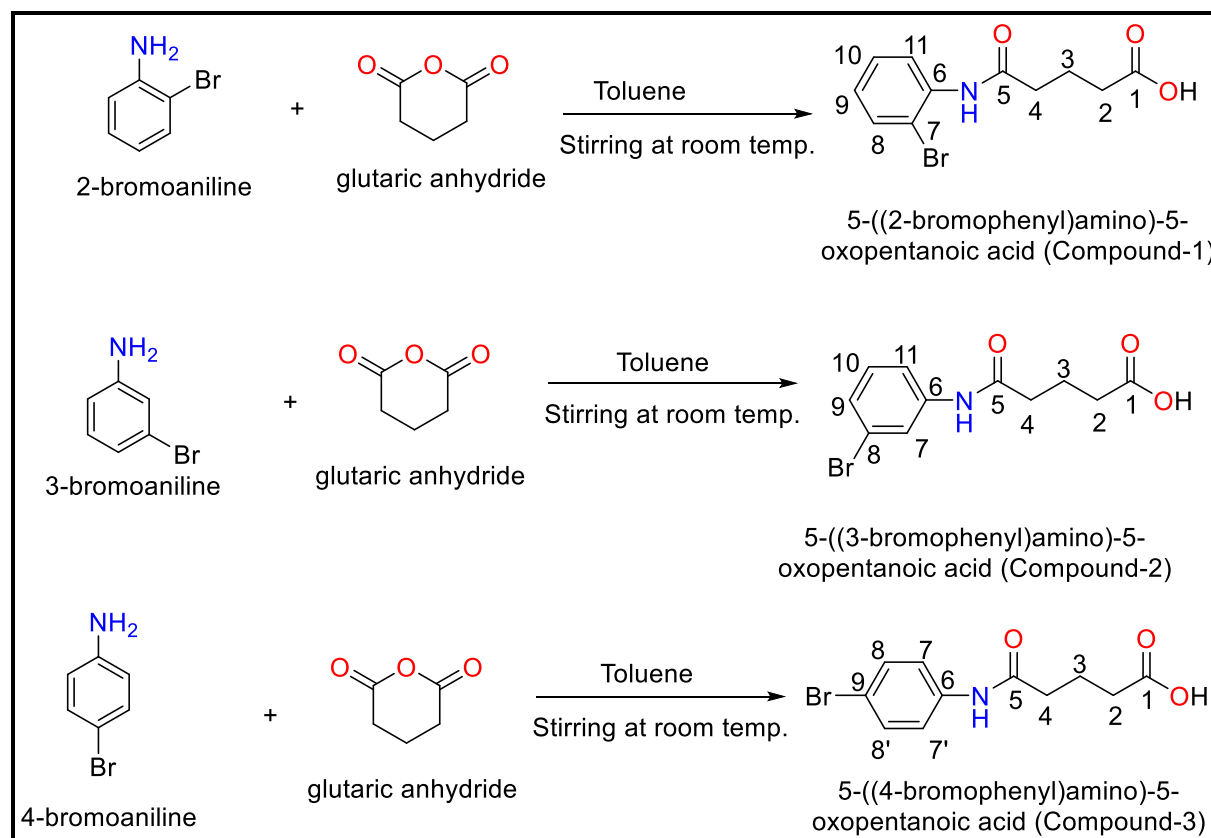
Compound	<b>1</b>	<b>2</b>	<b>3</b>
Formula	C <sub>11</sub> H <sub>12</sub> BrNO <sub>3</sub>	C <sub>11</sub> H <sub>12</sub> BrNO <sub>3</sub>	C <sub>11</sub> H <sub>12</sub> BrNO <sub>3</sub>
Formula weight	286.13	286.13	286.13
Crystal system	triclinic	triclinic	monoclinic
Space group	<i>P</i> 1	<i>P</i> 1	<i>P</i> 2 <sub>1</sub> / <i>c</i>
<i>a</i> (Å)	4.8317(2)	4.9260(2)	24.6256(2)
<i>b</i> (Å)	10.2446(6)	8.3664(5)	4.80980(5)
<i>c</i> (Å)	12.0871(7)	14.6791(6)	9.79495(13)
$\alpha$ (°)	93.050(5)	98.247(4)	90
$\beta$ (°)	98.725(4)	96.176(3)	97.4563(10)
$\gamma$ (°)	99.408(4)	99.697(4)	90
<i>V</i> (Å <sup>3</sup> )	581.55(5)	584.75(5)	1150.34(2)
<i>Z</i>	2	2	4
<i>D</i> <sub>x</sub> (g cm <sup>-3</sup> )	1.634	1.625	1.652
<i>F</i> (000)	288	288	576
$\mu$ (mm <sup>-1</sup> )	4.774	4.748	4.827
Reflections:			
collected	4094	12804	17562
unique ( <i>R</i> <sub>int</sub> )	2256 (0.032)	2078 (0.040)	2383 (0.033)
with <i>I</i> > 2 $\sigma$ ( <i>I</i> )	2101	1918	2289
<i>R</i> ( <i>F</i> ) [ <i>I</i> > 2 $\sigma$ ( <i>I</i> )]	0.042	0.041	0.033
<i>wR</i> ( <i>F</i> <sup>2</sup> ) [ <i>I</i> > 2 $\sigma$ ( <i>I</i> )]	0.116	0.107	0.094
<i>a</i> , <i>b</i> in weighting scheme	0.078, 0.162	0.047, 0.659	0.052, 0.577
<i>R</i> ( <i>F</i> ) [all data]	0.045	0.044	0.034
<i>wR</i> ( <i>F</i> <sup>2</sup> ) [all data]	0.118	0.110	0.095
Goodness of fit	1.07	1.06	1.06
max/min $\Delta\rho$ (e·Å <sup>-3</sup> )	0.37/-0.79	0.92/-0.93	0.49/-0.52
CCDC number	2111806	2115862	2111807

## 2.2 Synthesis

Glutaric anhydride (1.141 g, 10 mmol) dissolved in toluene (25 mL) was reacted with the respective *n*-bromoaniline (1.720 g, 10 mmol) also taken in toluene (25 mL) at room temperature. After the mixing two reactants, each precipitate appeared after a few minutes mixing, as depicted in Scheme 1. The precipitate was washed with toluene to remove any unreacted reactants and then



with distilled H<sub>2</sub>O to remove any glutaric acid. The product was then air dried to get the desired compound, **1-3** [18-23]. Recrystallization of each compound was from its acetone/ethanol (1:1 v/v) solution.



**Scheme 1:** Schematic representation of the reactions to give **1-3** along with atom numbering for NMR data interpretation

### 2.2.1 4-[(2-bromophenyl) carbamoyl]butanoic acid (1)

Melting point: 138-140 °C. Color: Red. Molecular formula: C<sub>11</sub>H<sub>12</sub>BrNO<sub>3</sub>. Molecular Weight: 286.13. **CHN** data in % (calculated/found): 46.18/46.36 (C); 4.23/4.16 (H); 4.90/4.87 (N). **FTIR** data (ν cm<sup>-1</sup>): 3275 (NH stretching); 2888 (H-bonded OH of the carboxylic moiety); 1689 (COO stretching); 1649 (amide carbonyl); 1578 (C=C); 1461 (OH bending); 1437 (COO bending) 1261 (NH bending); 1028 (C-N stretching). **<sup>1</sup>HNMR** (DMSO-d<sub>6</sub>, 500 MHz) with chemical shift in ppm: 11.00, s (OH of carboxylic moiety); 9.45, s (NH of amide moiety); H-2, t (2.39, <sup>3</sup>J<sub>H-H</sub> = 7.0 Hz); H-3, quint. (1.83, <sup>3</sup>J<sub>H-H</sub> = 7.3 Hz); H-4, t (2.30, <sup>3</sup>J<sub>H-H</sub> = 7.3 Hz); H-8, d (7.56, <sup>3</sup>J<sub>H-H</sub> = 8.0 Hz); H-9, t (7.15, <sup>3</sup>J<sub>H-H</sub> = 7.3 Hz); H-10, t (7.36, <sup>3</sup>J<sub>H-H</sub> = 7.5 Hz); H-11, d (7.64, <sup>3</sup>J<sub>H-H</sub> = 8.0 Hz). **<sup>13</sup>CNMR** (DMSO-d<sub>6</sub>, 125 MHz) with chemical shift in ppm: 174.6 (C-1); 35.3 (C-2); 21.0 (C-3); 33.5 (C-

1  
2  
3  
4 4); 171.4 (C-5); 136.8 (C-6); 118.8 (C-7); 133.1 (C-8); 128.0 (C-9); 128.4 (C-10); 127.5 (C-11).  
5  
6 MS:  $[M]^+$ : 285 m/e ( $^{79}\text{Br}$ ); base peak ( $[\text{C}_6\text{H}_6\text{NBr}]^+$ ): 171 m/e ( $^{79}\text{Br}$ ).  
7  
8

### 9 10 **2.2.2 4-[(3-bromophenyl) carbamoyl]butanoic acid (2)**

11 Melting point: 130-132 °C. Color: Red-brown. Molecular formula:  $\text{C}_{11}\text{H}_{12}\text{BrNO}_3$ . Molecular  
12 Weight: 286.13. **CHN** data in % (calculated/found): 46.18/46.20 (C); 4.23/4.20 (H); 4.90/4.92 (N).  
13 **FTIR** data ( $\nu \text{ cm}^{-1}$ ): 3295 (NH stretching); 2882 (H-bonded OH of the carboxylic moiety); 1688  
14 (COO stretching); 1656 (amide carbonyl); 1583 (C=C); 1476 (OH bending); 1438 (COO bending)  
15 1260 (NH bending); 1066 (C-N stretching).  **$^1\text{HNMR}$**  (DMSO- $d_6$ , 500 MHz) with chemical shift  
16 in ppm: 12.07, s (OH of carboxylic moiety); 10.06, s (NH of amide moiety); H-2, t (2.36,  $^3J_{\text{H-H}} =$   
17 7.0 Hz); H-3, quint. (1.81,  $^3J_{\text{H-H}} = 7.0$  Hz); H-4, t (2.26,  $^3J_{\text{H-H}} = 7.5$  Hz); H-7, s (7.96); H-9, d (7.47,  
18  $^3J_{\text{H-H}} = 7.0$  Hz); H-10, t (7.25,  $^3J_{\text{H-H}} = 7.5$  Hz); H-11, d (7.21,  $^3J_{\text{H-H}} = 7.0$  Hz).  **$^{13}\text{CNMR}$**  (DMSO-  
19  $d_6$ , 125 MHz) with chemical shift in ppm: 174.6 (C-1); 35.7 (C-2); 20.8 (C-3); 33.4 (C-4); 171.6  
20 (C-5); 141.3 (C-6); 121.8 (C-7); 122.0 (C-8); 126.0 (C-9); 131.1 (C-10); 118.2 (C-11). MS:  $[M]^+$ :  
21 285 m/e ( $^{79}\text{Br}$ ); base peak ( $[\text{C}_6\text{H}_6\text{NBr}]^+$ ): 171 m/e ( $^{79}\text{Br}$ ).  
22  
23  
24  
25  
26  
27  
28  
29  
30  
31  
32

### 33 34 **2.2.3 4-[(3-bromophenyl) carbamoyl]butanoic acid (3)**

35 Melting point: 160-162 °C. Color: Red-brown. Molecular formula:  $\text{C}_{11}\text{H}_{12}\text{BrNO}_3$ . Molecular  
36 Weight: 286.13. **CHN** data in % (calculated/found): 46.18/46.95 (C); 4.23/4.10 (H); 4.90/5.01 (N).  
37 **FTIR** data ( $\nu \text{ cm}^{-1}$ ): 3307 (NH stretching); 2894 (H-bonded OH of the carboxylic moiety); 1689  
38 (COO stretching); 1662 (amide carbonyl); 1586 (C=C); 1485 (OH bending); 1436 (COO bending);  
39 1271 (NH bending); 1010 (C-N stretching).  **$^1\text{HNMR}$**  (DMSO- $d_6$ , 500 MHz) with chemical shift  
40 in ppm: 12.08, s (OH of carboxylic moiety); 10.03, s (NH of amide moiety); H-2, t (2.35,  $^3J_{\text{H-H}} =$   
41 7.5 Hz); H-3, quint. (1.80,  $^3J_{\text{H-H}} = 7.5$  Hz); H-4, t (2.27,  $^3J_{\text{H-H}} = 7.3$  Hz); H-7,7', d (7.56,  $^3J_{\text{H-H}} =$   
42 9.0 Hz); H-8,8', d (7.46,  $^3J_{\text{H-H}} = 8.0$  Hz).  **$^{13}\text{CNMR}$**  (DMSO- $d_6$ , 125 MHz) with chemical shift in  
43 ppm: 174.6 (C-1); 35.8 (C-2); 20.8 (C-3); 33.4 (C-4); 171.4 (C-5); 139.0 (C-6); 121.4 (C-7,7');  
44 131.9 (C-8,8'); 114.9 (C-9). MS:  $[M]^+$ : 285 m/e ( $^{79}\text{Br}$ ); base peak ( $[\text{C}_6\text{H}_6\text{NBr}]^+$ ): 171 m/e ( $^{79}\text{Br}$ ).  
45  
46  
47  
48  
49  
50  
51  
52  
53  
54  
55

## 56 **2.3 Antimicrobial screening**

57 The antibacterial data were determined against five bacterial strains, as specified in Table 2. All  
58 bacteria were cultured in Cation-adjusted Mueller Hinton broth (CAMHB) at 37 °C overnight. A  
59  
60  
61  
62  
63  
64  
65

1  
2  
3  
4 sample of each culture was then diluted 40-fold in fresh broth and incubated at 37 °C for 1.5-3 h.  
5  
6 The resultant mid-log phase cultures were diluted then added to each well of the compound  
7  
8 containing plates, giving a cell density of  $5 \times 10^5$  CFU/mL. Plates were covered and incubated at  
9  
10 37 °C for 18 h without shaking. Inhibition of bacterial growth was determined measuring  
11  
12 absorbance at 600 nm (OD600), using a Tecan M1000 Pro monochromator plate reader (Equipped  
13  
14 with premium quad4 monochromators). The percentage of growth inhibition was calculated for  
15  
16 each well, using the negative control (media only) and positive control (bacteria without inhibitors)  
17  
18 on the same plate as references. For the screening, the significance of the inhibition values was  
19  
20 determined by modified Z-scores, calculated using the median and mean absolute deviation  
21  
22 (MAD) of the samples (no controls) on the same plate. Samples with inhibition value above 80%  
23  
24 and Z-Score  $> 2.5$  for either replicate (n=2 on different plates) were classed as actives while sample  
25  
26 with inhibition below 50.9% - 79.9% and Z-Score  $< 2.5$  were classed as inactive [24].

27  
28 The antifungal data was collected against two fungal strains as detailed in Table 2. Fungi  
29  
30 strains were cultured for 3 days on Yeast Extract-Peptone Dextrose (YPD) agar at 30 °C. A yeast  
31  
32 suspension of  $1 \times 10^6$  to  $5 \times 10^6$  CFU/mL (as determined by OD530) was prepared from five  
33  
34 colonies. The suspension was subsequently diluted and added to each well of the compound-  
35  
36 containing plates giving a final cell density of fungi suspension of  $2.5 \times 10^3$  CFU/mL and a total  
37  
38 volume of 50  $\mu$ L. All plates were covered and incubated at 35 °C for 24 h without shaking. Growth  
39  
40 inhibition of *C. albicans* was determined measuring absorbance at 530 nm (OD530), while the  
41  
42 growth inhibition of *C. neoformans* was determined measuring the difference in absorbance  
43  
44 between 600 and 570 nm (OD600-570), after the addition of resazurin (0.001% final  
45  
46 concentration) and incubation at 35 °C for additional 2 h. The absorbance was measured using a  
47  
48 Biotek Synergy HTX plate reader (Light source: Xenon flash lamp Detector: Photodiode  
49  
50 Wavelength selection: Monochromator Wavelength range: 200 – 999 nm, 1 nm increments  
51  
52 Monochromator bandwidth: 2.4 nm Dynamic range: 0 – 4.0 OD Resolution: 0.0001 OD Pathlength  
53  
54 correction: Yes Monochromator wavelength accuracy:  $\pm 2$  nm Monochromator wavelength  
55  
56 repeatability:  $\pm 0.2$  nm OD linearity). The percentage of growth inhibition was calculated for each  
57  
58 well, using the negative control (media only) and positive control (bacteria without inhibitors) on  
59  
60 the same plate as references [24].

61  
62 Colistin and Vancomycin were used as positive bacterial inhibitor standards for Gram-negative and  
63  
64 Gram-positive bacteria, respectively. Fluconazole was used as a positive fungal inhibitor standard  
65

for *C. albicans* and *C. neoformans*. The antibiotics were provided in 4 concentrations, with 2 above and 2 below its MIC value, and plated into the first 8 wells of column 23 of the 384-well NBS plates.

**Table 2**

Information of the bacterial and fungal strain and standards investigated in the present study

Abbr.	Code	Name	Description	Strain	Organism	Type
Sa	GP_020	<i>Staphylococcus aureus</i>	MRSA	ATCC 43300	Bacteria	G+ve
Ec	GN_001	<i>Escherichia coli</i>	FDA control	ATCC 25922	Bacteria	G-ve
Kp	GN_003	<i>Klebsiella pneumoniae</i>	MDR	ATCC 700603	Bacteria	G-ve
Ab	GN_034	<i>Acinetobacter baumannii</i>	Type strain	ATCC 19606	Bacteria	G-ve
Pa	GN_042	<i>Pseudomonas aeruginosa</i>	Type strain	ATCC 27853	Bacteria	G-ve
Ca	FG_001	<i>Candida albicans</i>	CLSI reference	ATCC 90028	Fungi	Yeast
Cn	FG_002	<i>Cryptococcus neoformans var. grubii</i>	Type strain	H99; ATCC 208821	Fungi	Yeast
Standards						
Sample name	Sample ID	Full MW	Stock Conc. (mg/mL)	Solvent	Source	
Colistin-Sulfate	MCC_000094:02	1400.63	10.0	DMSO	Sigma; C4461	
Vancomycin-HCL	MCC_000095:02	485.71	10.0	DMSO	Sigma; 861987	
Fluconazole	MCC_008383:01	306.27	2.56	DMSO	Sigma; F8929	

#### 2.4 DNA binding assay by UV-visible spectroscopy and viscometry

A solution of Salmon sperm DNA was prepared in distilled water by dissolving 2 mg of the sodium salts of SS-DNA and stirred at room temperature overnight. The concentration of the solution was determined on a UH-5300 UV/Vis. spectrophotometer using based on  $\epsilon = 6600 \text{ M}^{-1} \cdot \text{cm}^{-1}$  and found

1  
2  
3  
4 to be  $1.4 \times 10^{-4}$  M. The nature of DNA free from protein was checked from its absorbance ratio  
5  $A_{260}/A_{280} = 1.8$ . A solution of each of **1-3** (1 mM) was prepared in 70% absolute EtOH. During  
6 the DNA binding study, the concentration of **1-3** was kept constant while that of the DNA was  
7 changed [25-27].  
8  
9

10  
11 The viscosity was measured at a temperature of  $29 \pm 1$  °C using an Ubbelohde viscometer.  
12 A digital timer was used to measure the flow time. The average flow time was determined after  
13 measuring each sample three times. The results were shown as a plot of relative viscosity  
14  $[(\eta/\eta_0)^{1/3}]$ , vs. binding ratio  $[(\text{compound})/(\text{DNA})]$ , where  $\eta$  indicates the viscosity of DNA in the  
15 presence of **1-3** and  $\eta_0$  the viscosity of DNA only. Viscosity results were determined from the  
16 experimental flow rate of DNA containing solution,  $\eta = t - t_0$  [28-30].  
17  
18  
19  
20  
21  
22  
23

## 24 **2.5 DPPH scavenging activity**

25  
26 DPPH (3.94 mg) was dissolved in MeOH (100 mL). The DPPH and solutions of **1-3** were prepared  
27 as follows: to methanolic solutions of DPPH (2800  $\mu\text{L}$ ) was added 0.2  $\mu\text{L}$  of **1-3** (also prepared in  
28 methanol) with concentrations of **1-3** ranging from 10 to 150 mg/mL. The decrease in DPPH  
29 absorbance was noted at 517 nm after 10 min *via* UV-visible spectrophotometer (provide details).  
30 The same protocol was followed for well-known antioxidant, ascorbic acid, as a control. All the  
31 measurements were performed in triplicate and average results reported. The percent scavenging  
32 activity of screened compounds was measured as per [31-33]:  
33  
34  
35  
36  
37  
38

$$39 \quad \% \text{ Scavenging activity} = \frac{A_o - A_s}{A_o}$$

40  
41  
42  $A_o$  and  $A_s$  represent the DPPH absorbance in the absence (control) and presence of sample (**1-3**),  
43 respectively.  
44  
45  
46

## 47 **2.6 Drug-likeness and ADME studies**

48  
49 ADME properties such as physicochemical and pharmacokinetics of the synthesized compounds  
50 and drug similarity properties were performed on the SwissADME webserver [34, 35]. These  
51 studies provide properties such as TPSA, molecular weight, hydrogen bond acceptor/donor atoms  
52 and lipophilicity (logP). A BOILED-Egg model of the compounds, the absorption in the  
53 gastrointestinal system and the crossing of the blood-brain barrier were also evaluated [36]. The  
54 oral bioavailability of the compounds was also examined on six parameters employing a radar  
55  
56  
57  
58  
59  
60  
61  
62  
63  
64  
65

1  
2  
3  
4 image. Drug-likeness analysis of the compounds, “Lipinski's Rule of Five” compatibility was  
5 examined using the same SwissADME webserver [34, 35].  
6  
7  
8

### 9 10 **3 Results and Discussion**

11 Three new isomeric 4-[(n-bromophenyl)carbamoyl]butanoic acids (n = 2, 3, and 4) compounds, **1-**  
12 **3**, have been synthesized from the 1:1 (nucleophilic addition) reaction of glutaric anhydride with  
13 respective n-bromoaniline. The lone pair of electrons on the N atom of the n-bromoaniline attack  
14 on the electrophilic carbonyl carbon of the glutaric anhydride, followed by the abstraction of H<sup>+</sup>  
15 from the electropositive N atom by the negatively charged oxygen atom resulting in the formation  
16 of the desired 4-[(n-bromophenyl)carbamoyl]butanoic acids [37, 38]. The compounds are air  
17 stable, soluble in common organic solvents including MeOH, EtOH, DMSO, acetone and  
18 chloroform. Details of the spectroscopic and crystallographic characterization are given below. In  
19 addition, certain medicinal potential, namely DNA binding, antimicrobial, antioxidant potentials,  
20 and the theoretical determination of medicinally relevant attributes are reported.  
21  
22  
23  
24  
25  
26  
27  
28  
29  
30

#### 31 **3.1 FTIR**

32 The FTIR spectra of **1-3** were recorded in the range 4000–450 cm<sup>-1</sup>. A broad peak of weak intensity  
33 centered at 2888, 2882, 2894 cm<sup>-1</sup> for **1-3**, respectively, is attributed to the hydrogen bonded O–H  
34 stretching vibrations of the carboxylic acid. The strong N–H stretching appeared at 3275, 3295,  
35 and 3307 cm<sup>-1</sup> for **1-3**, respectively, while the N–H bending vibration were observed at 1261, 1260,  
36 and 1271 cm<sup>-1</sup>, respectively. A peak at 1649, 1656, and 1662 cm<sup>-1</sup> was assigned to the amide  
37 carbonyl stretching in **1-3**. A medium intensity peak at 1028, 1066, and 1010 cm<sup>-1</sup> is attributed to  
38 the C–N stretching vibration, while the asymmetric COO stretching band appeared as a strong  
39 peak at 1689, 1688, and 1689 cm<sup>-1</sup> in **1-3** [19, 20].  
40  
41  
42  
43  
44  
45  
46  
47  
48  
49

#### 50 **3.2 NMR**

51 The <sup>1</sup>H NMR spectra of **1-3** displayed a singlet resonance at 12.07, 11.00, and 12.08 ppm,  
52 respectively, which is assigned to the carboxylic acid OH confirming the presence of the  
53 carboxylic acid residue in each case. Similarly, another characteristic resonance is ascribed to the  
54 NH proton i.e., a singlet in the range 9.45-10.03 ppm. Additional resonances, multiplicity and  
55 integration, are as expected, see **2.2.1 – 2.2.3**.  
56  
57  
58  
59  
60  
61  
62  
63  
64  
65

1  
2  
3  
4 The most notable features in the  $^{13}\text{C}$  NMR spectra of the compounds **1-3** were downfield  
5 resonances at  $\delta$  174.6 ppm (**1-3**) and at  $\delta$  171.4, 171.6, and 171.4 ppm, which are assigned to the  
6 carboxylic acid (C-1) and amide (C-4) nuclei. The resonances of the remaining nuclei fall in their  
7 anticipated regions [19, 20], as detailed in **2.2.1 – 2.2.3**.  
8  
9

### 10 11 12 13 **3.3 X-ray crystallography**

14  
15 The crystal and molecular structures of isomeric **1-3** have been established by X-ray  
16 crystallography. The molecular structures are illustrated in Figure 1 and selected geometric  
17 parameters are collated in Table 3. The three molecules differ in the position of the bromide  
18 substituent in the terminal phenyl ring, and bear a close resemblance to each other so the discussion  
19 will focus on the 2-bromo derivative, **1**. Evidence for the carboxylic acid assignment is readily  
20 gained through the large difference between the C–O1, O2 bond lengths, Table 3, and in the pattern  
21 of supramolecular association between molecules (see below); the angles subtended at the C1 atom  
22 involving the O2 atom are wider, again consistent with the presence of a C1=O2 bond. The bond  
23 lengths in the amide functionality, which adopts an anti-conformation, are as expected and the  
24 angles at C5 involving the carbonyl-O5 atom are systematically wider. Based on the torsion angle  
25 data included in Table 3, there is a kink in the chain linking the carboxylic acid and amide residues.  
26 The twist occurs about the C4–C5 bond with the torsion angle ( $-145.3(3)^\circ$ ) indicative of a -anti-  
27 clinal (-ac) conformation. A second twist in the molecule occurs about the C6–N1 bond, consistent  
28 with a +anti-clinal (-ac) conformation.  
29  
30  
31  
32  
33  
34  
35  
36  
37  
38  
39  
40  
41  
42  
43  
44  
45  
46  
47  
48  
49  
50  
51  
52  
53  
54  
55  
56  
57  
58  
59  
60  
61  
62  
63  
64  
65

1  
2  
3  
4  
5  
6  
7  
8  
9  
10  
11  
12  
13  
14  
15  
16  
17  
18  
19  
20  
21  
22  
23  
24  
25  
26  
27  
28  
29  
30  
31  
32  
33  
34  
35  
36  
37  
38  
39  
40  
41  
42  
43  
44  
45  
46  
47  
48  
49  
50  
51  
52  
53  
54  
55  
56  
57  
58  
59  
60  
61  
62  
63  
64  
65

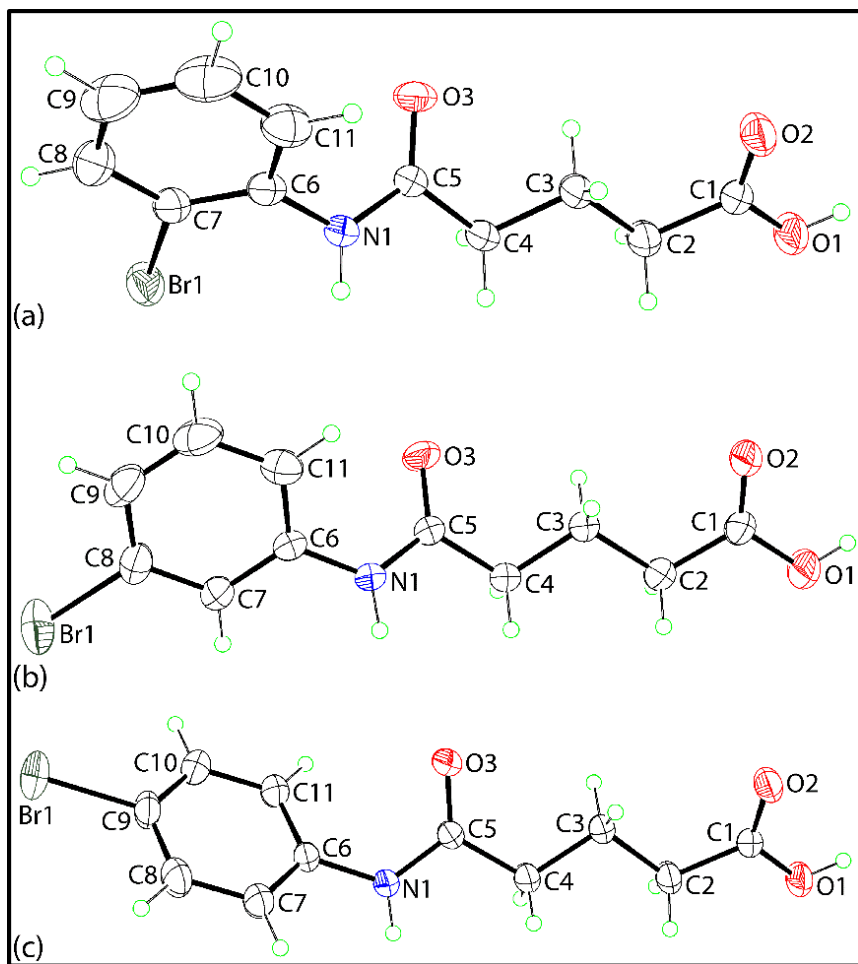


**Fig. 1.** The molecular structures of (a) **1**, (b) **2**, and (c) **3**, showing the atom-labelling scheme and displacement ellipsoids at the 35% probability level.



**Table 3**Selected geometric parameters (Å, °) for **1-3**

Parameter	<b>1</b>	<b>2</b>	<b>3</b>
C1–O1	1.311(4)	1.307(4)	1.302(2)
C1–O2	1.213(4)	1.211(4)	1.232(2)
C5–O3	1.218(4)	1.221(3)	1.218(2)
C5–N1	1.340(4)	1.343(4)	1.350(2)
C6–N1	1.417(4)	1.416(4)	1.422(2)
C5–N1–C6	122.8(2)	125.3(2)	124.68(16)
O1–C1–O2	123.5(3)	123.0(3)	123.49(17)
O1–C1–C2	113.0(3)	113.2(3)	113.61(17)
O2–C1–C2	123.5(3)	123.8(3)	122.87(18)
O3–C5–N1	122.9(3)	122.8(3)	122.68(18)
O3–C5–C4	120.7(3)	121.5(3)	123.25(18)
N1–C5–C4	116.3(2)	115.8(2)	114.06(16)
C1–C2–C3–C4	-177.7(3)	-175.6(3)	-171.5(2)
C2–C3–C4–C5	-176.6(3)	176.2(3)	-173.3(2)
C3–C4–C5–N1	-145.3(3)	-141.1(3)	-171.4(2)
C4–C5–N1–C6	177.1(3)	-177.9(3)	178.7(2)
C5–C6–N1–C7	127.5(3)	135.5(3)	-135.0(2)
CO <sub>2</sub> /C <sub>6</sub>	14.3(3)	8.0(3)	75.83(11)

The molecular structure of **2** mimics that just described for **1**, an observation entirely consistent with the isostructural relationship between the crystals, Table 1. While the bond lengths and angles in **3** match those of the previous isomers, a difference in the chain is noted with the C3–C4–C5–N1 torsion angle (-171.4(2)°) indicative of a -anti-periplanar (-ap) conformation. In addition to the difference in the conformation of the side-chains, the dihedral angle between the terminal carboxylic acid and phenyl residues is close to perpendicular in **3** in contrast the those in **1** and **2**. The conformational differences between the three molecules are highlighted in Figure 2. The conformational flexibility of related molecules has already been noted in the literature [22, 23].

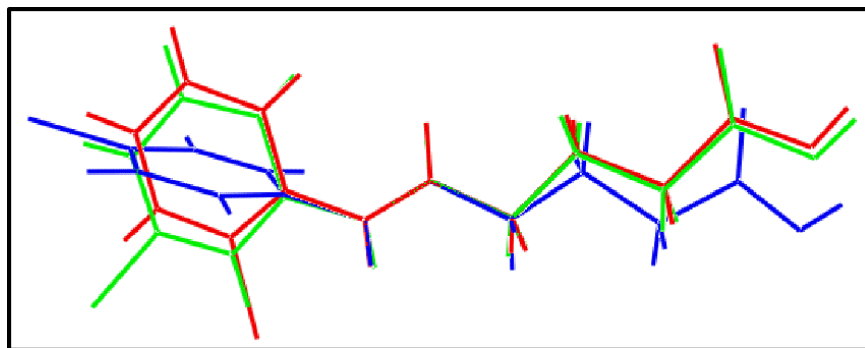


**Fig. 2.** An overlay diagram of **1** (red image), **2** (green image), and **3** (blue image), highlighting the similarity in the conformations of **1** and **2**, and the difference between these and that of **3**. The molecules have been overlapped so the amide residues are coincident.

As anticipated from the chemical composition of **1-3**, conventional hydrogen bonding interactions are prominent in the supramolecular association in their crystals. Indeed, all three crystals feature comparable hydrogen bonding patterns, namely the self-association of the carboxylic acid residues about a center of inversion to generate eight-membered  $\{\dots\text{OCOH}\}_2$  synthons, and the subsequent linking of the dimeric aggregates into tapes via amide-N-H...O(amide) hydrogen bonds; geometric data characterizing the specified contacts are included in Table 3. A representative tape is shown in Figure 3a for **1**. Also shown is a side-on view which indicates a significant deviation from planarity in the tape. A similar situation pertains for isostructural **2**, Figure 3b, in contrast to the near to planar tape noted in the crystal of **3**, Figure 3c.

**Table 4**Hydrogen bonding (A–H...B) interactions in the crystals of **1-3**

A	H	B	H...B (Å)	A...B (Å)	A–H...B (°)	Symmetry operation
<b>1</b>						
O1	H1o	O2	1.86	2.679(3)	174	1-x, 2-y, 2-z
N1	H1n	O3	2.15	2.983(4)	164	1+x, y, z
<b>2</b>						
O1	H1o	O2	1.86(5)	2.680(4)	178(7)	2-x, 1-y, 2-z
N1	H1n	O3	2.119(18)	2.963(3)	169(3)	-1+x, y, z
<b>3</b>						
O1	H1o	O2	1.84	2.653(2)	172	1-x, 1-y, 2-z
N1	H1n	O3	2.20	3.028(2)	160	x, 1+y, z

Based on an assessment of the molecular packing employing PLATON [17], the tapes in the crystal of **1** assemble without directional interactions between them. There is evidence of a close Br1...Br1<sup>i</sup> contact in the crystal of **2** with the separation being 3.6097(7) Å, close to the sum of the van der Waals radii of 3.70 Å [17]; symmetry operation (i): -x, -y, -z. This interaction has the character of a type-I halogen bonding contact which often equates to a van der Waals contact arising a result of global molecular packing considerations rather than being a directional interaction. In continuation of the theme of a lack of directional interactions between the supramolecular tapes in **1-3**, Br...Br contacts are evident in the crystal of **3** but, with the Br1...Br1<sup>ii</sup> separations are longer than the sum of the van der Waals radii, with the separation being 3.7552(6) Å; symmetry operation (ii): 2-x, -1/2+y, 1/2-z.

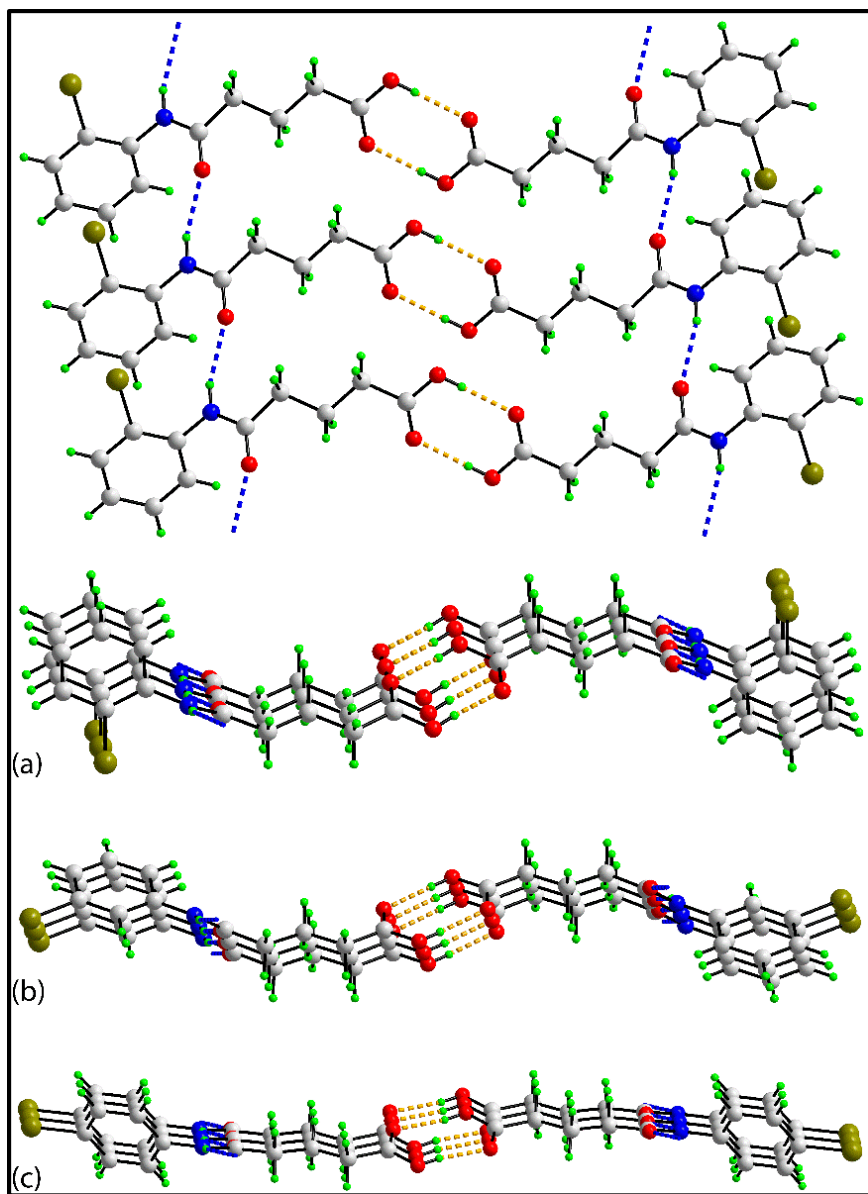
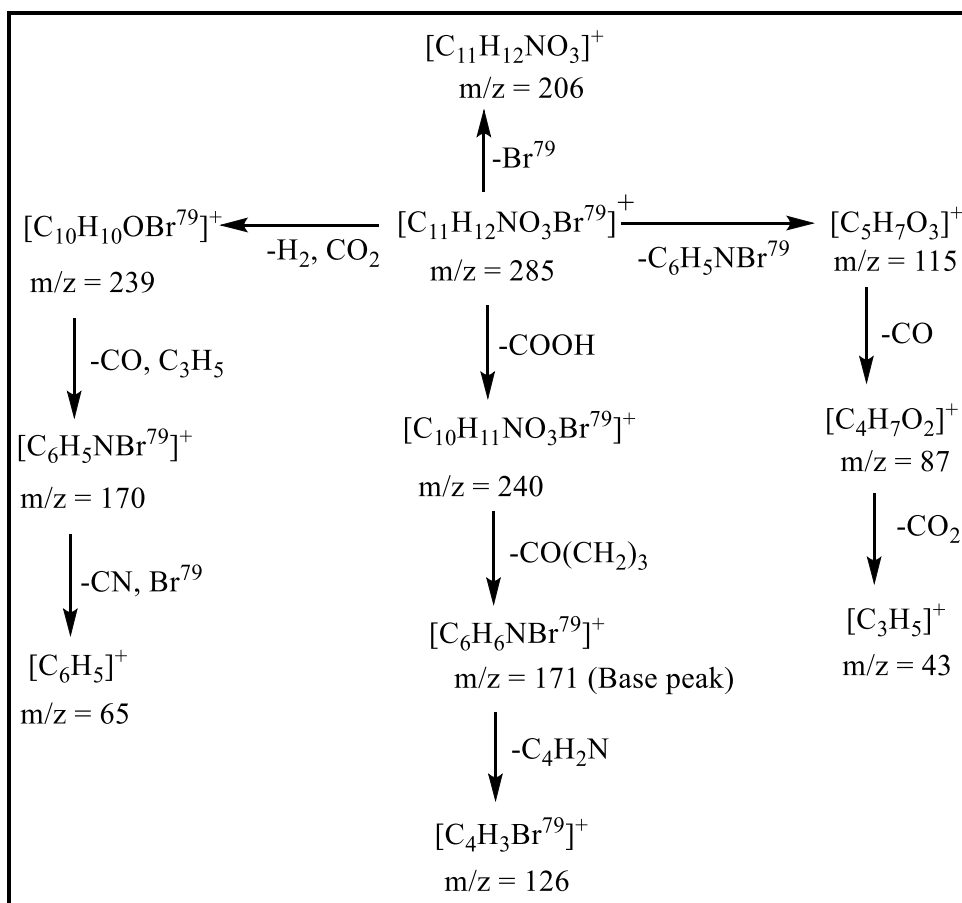


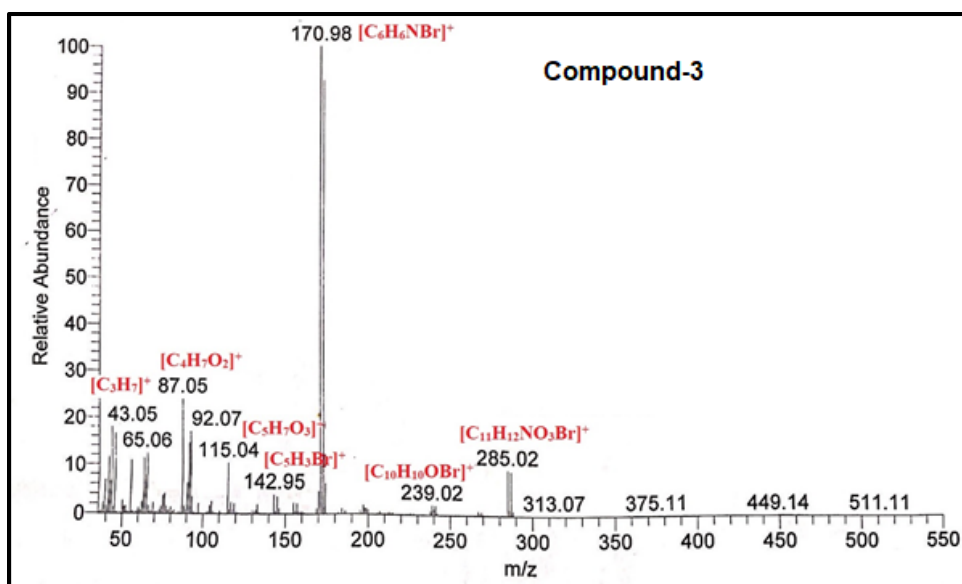
**Fig. 3.** Supramolecular tapes in (a) **1**, plan and side-on views, (b) **2**, side-on view, and (c) **3**, side-on.

### 3.4 Mass spectrometry

Mass spectral data for isomeric **1-3** were obtained by electron impact (EI) at 70 eV. As anticipated from the isomeric composition, the general mass fragmentation patterns are similar and are summarized in Scheme 2, with a representative mass spectrum for **3** shown in Figure 4. The molecular ion peak  $[M]^+$  with isotopic  $^{79}\text{Br}$  was noted at  $m/z = 285$ , and the molecular ion peak loses the  $\text{COOH}$  and  $\text{CO}(\text{CH}_2)_3$  units to give the baseline peak at  $m/z = 171$ .



35 Scheme 2. General mass fragmentation pattern for compounds 1-3



58 Fig. 4. Mass spectrum for 3.

### 3.5 Antimicrobial activity

Compounds **1-3**, being soluble in DMSO, were submitted to CO-ADD (the Community for Open Antimicrobial Drug Discovery). The compounds undergo a primary screen in duplicate at a single concentration (32  $\mu\text{g/mL}$ ) in 384-well format to test their killing ability against broth solutions of key ESKAPE bacterial pathogens: *S. aureus* (MRSA), *E. coli*, *K. pneumoniae*, *A. baumannii*, *P. aeruginosa*, and as well as fungal pathogens *C. neoformans* and *C. albicans*; see Table 2 for details. It can be seen from Table 5 that the maximum antibacterial activity exhibited by **1** and **2** is against *P. aeruginosa* while that of **3** shows is against *K. pneumoniae*. In terms of antifungal activity, all compounds were most active against the *C. neoformans* compared to *C. albicans*. The Z-score of the screened compounds against both bacterial and fungal strains was below  $|2.5|$ . Since the antimicrobial inhibition exhibited by **1-3** is lower than 50%, they are considered inactive. Accordingly, none of the compounds was selected for further dose response studies or Hit-confirmation.

**Table 5**

Percentage inhibition exhibited by **1-3** against selected bacteria and fungi<sup>a</sup>

Compd.	% Inhibition						
	Antibacterial				Antifungal		
	<i>S.</i> <i>aureus</i> (MRSA)	<i>E.</i> <i>coli</i>	<i>K.</i> <i>pneumoniae</i>	<i>P.</i> <i>aeruginosa</i>	<i>A.</i> <i>baumannii</i>	<i>C.</i> <i>albicans</i>	<i>C.</i> <i>neoformans</i>
<b>1</b>	-1.63	5.02	12.01	16.77	5.61	7.45	-20.86
<b>2</b>	0.16	2.41	10.89	13.32	11.44	5.25	-18.95
<b>3</b>	2.04	7.36	14.89	9.67	12.85	4.14	-13.51

<sup>a</sup> Active compound: Inhibition  $\geq 80\%$  and  $\text{abs}(\text{Z-Score}) > |2.5|$ . Partial Active: Inhibition = 50.9 – 79.9% and  $\text{abs}(\text{Z-Score}) < |2.5|$ . Inactive compounds: Inhibition  $< 50\%$  and  $\text{abs}(\text{Z-Score}) < |2.5|$

### 3.6 DNA interaction

The interactions between **1-3** and DNA were studied via UV-visible spectroscopic with the results summarized in Figures 5-7, respectively. Each compound exhibited two strong bands at approximately 200-230 and 235-300 nm ascribed to  $\pi-\pi^*$  and  $n-\pi^*$  transitions, respectively. Upon

1  
2  
3  
4 interaction with DNA, two phenomena were observed: hypochromism along with a bathochromic  
5 effect of 2-5 nm. After intercalating the base pairs of DNA, the  $\pi^*$  orbital of the intercalated  
6 molecule couples with the  $\pi$  orbital of the base pairs, thereby decreasing the  $\pi$ - $\pi^*$  transition energy,  
7 resulting in the bathochromic shift. Further, the coupling of the respective, partially filled  $\pi$  orbital  
8 decreases the transition probabilities resulting in the observed hypochromic shift. When these two  
9 phenomena occur then the dominant mode of interaction is the intercalation, which involves strong  
10 stacking between the chromophore and the base pairs of DNA [31-33]. The binding constant ( $K_b$ )  
11 was determined from the intercept to slope ratio of the plot of  $A_o/(A-A_o)$  vs.  $1/[DNA]$  as shown in  
12 the inset of Figures 5-7. The  $K_b$  value was then used to determine the Gibb's free energy value  
13 (which relates to the spontaneity of DNA-compound adduct formation) from the equation  $\Delta G = -$   
14  $RT \ln K_b$ , where the negative sign of  $\Delta G$  indicate the spontaneity of the DNA-compound adduct  
15 formation [31-33].  
16  
17  
18  
19  
20  
21  
22  
23  
24  
25

26 The intercalative binding mode of between **1-3** and DNA was further confirmed by the  
27 viscometric method. During the viscosity measurements, the viscosity of the DNA in the presence  
28 of various concentration of **1-3** was increased due to the entrance of the respective compound  
29 between the DNA bases resulting in the lengthening of DNA. The increase in the viscosity of DNA  
30 upon the addition of various concentration is the sign of the intercalative binding mode [34]. The  
31 plot of relative viscosity vs. ratio of the concentration of **1-3**/DNA is shown in Figure 8.  
32  
33  
34  
35  
36  
37  
38  
39  
40  
41  
42  
43  
44  
45  
46  
47  
48  
49  
50  
51  
52  
53  
54  
55  
56  
57  
58  
59  
60  
61  
62  
63  
64  
65

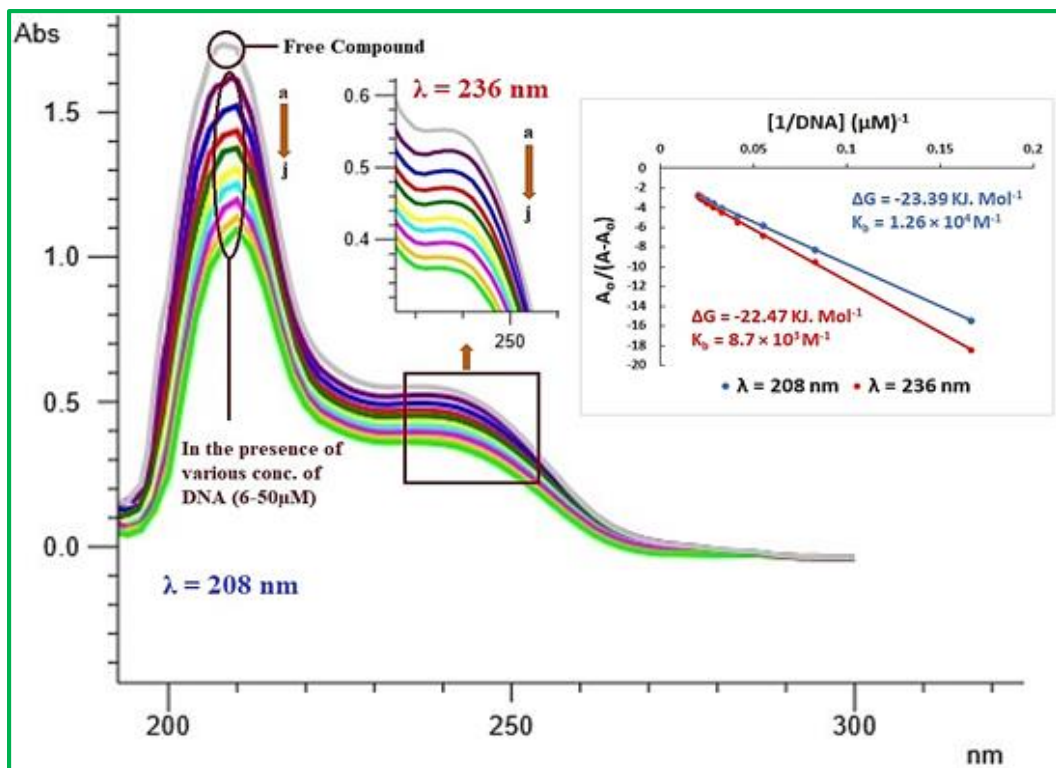
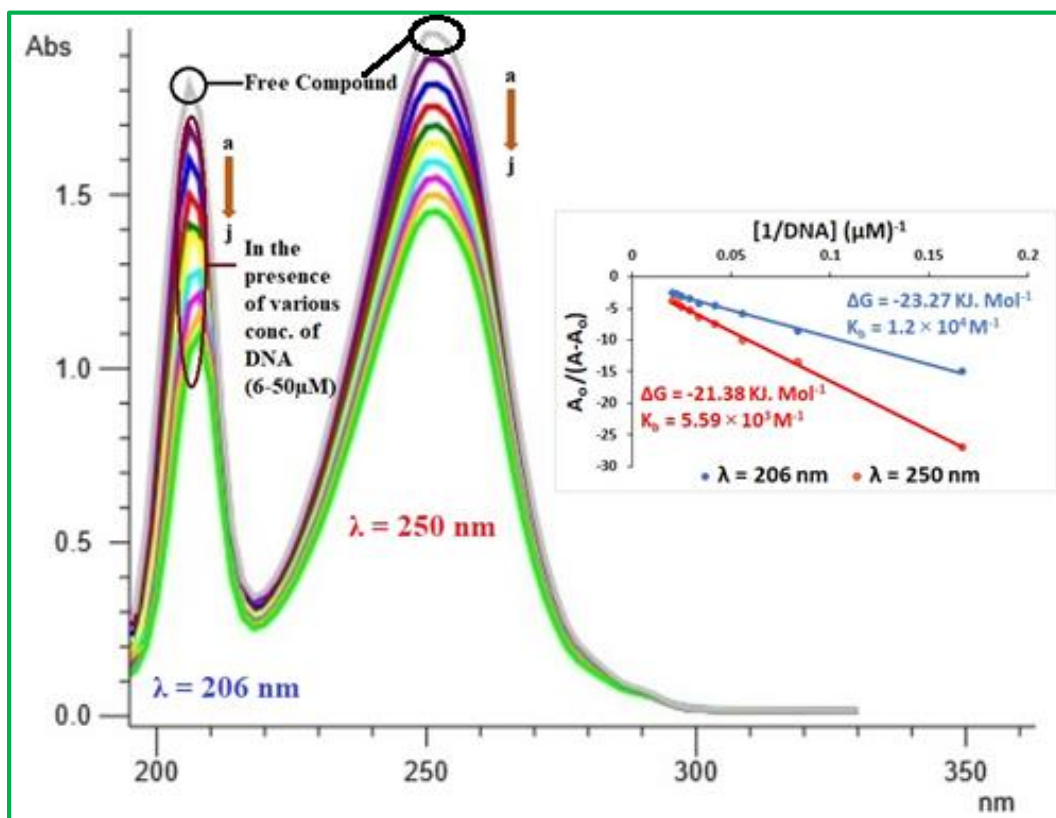
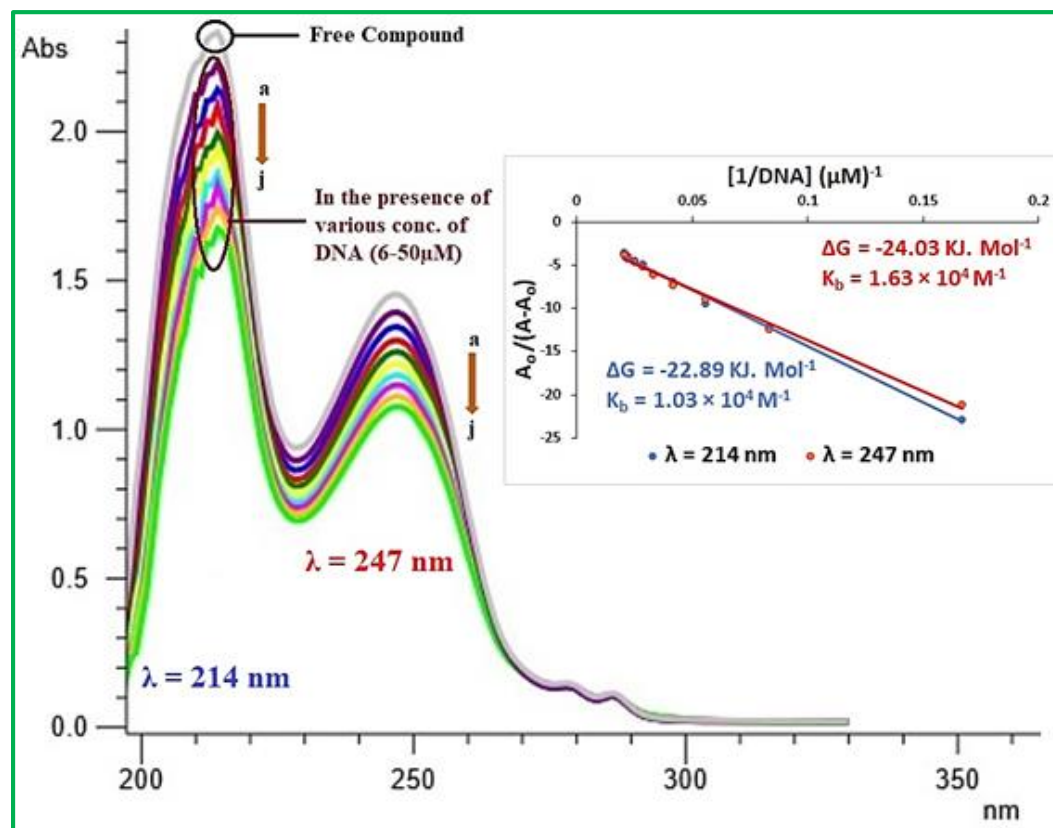


**Fig. 5.** DNA binding spectra of **1** (1 mM), in the absence and presence of various DNA concentrations. The arrowhead represents the increasing concentration of DNA.





1  
2  
3  
4 **Fig. 6.** DNA binding spectra of **2** (1 mM), in the absence and presence of various DNA  
5 concentrations. The arrowhead represents the increasing concentration of DNA.  
6  
7



35  
36 **Fig. 7.** DNA binding spectra of **3** (1 mM), in the absence and presence of various DNA  
37 concentrations. The arrowhead represents the increasing concentration of DNA.  
38  
39  
40  
41  
42  
43  
44  
45  
46  
47  
48  
49  
50  
51  
52  
53  
54  
55  
56  
57  
58  
59  
60  
61  
62  
63  
64  
65

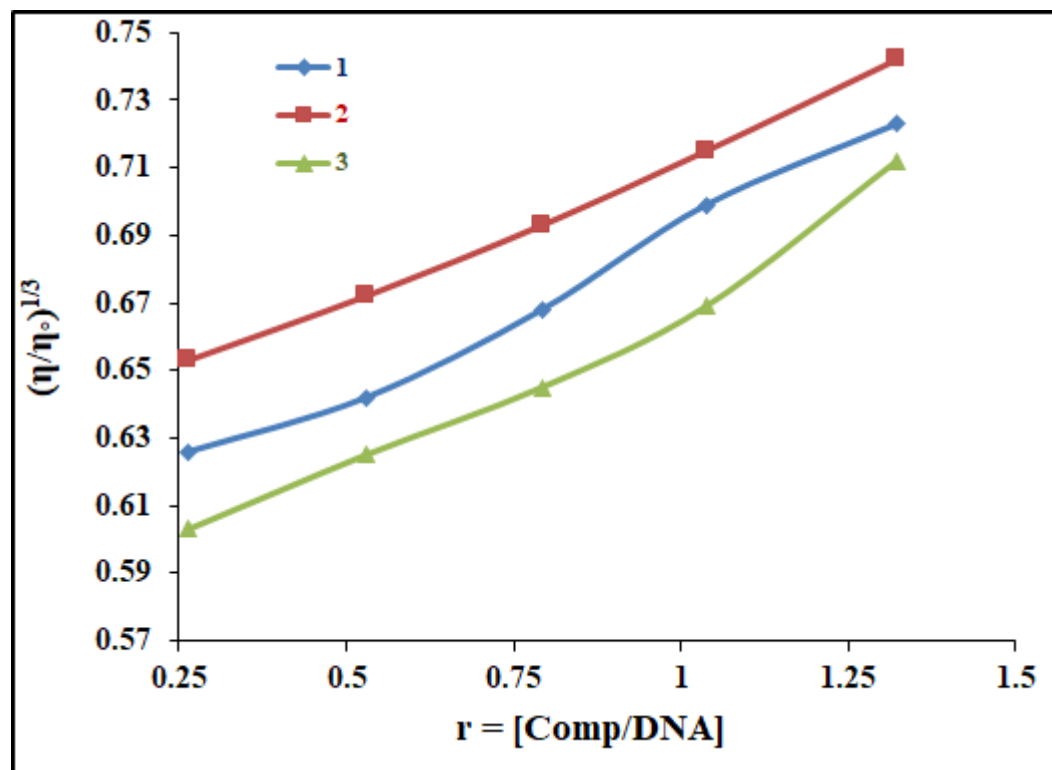
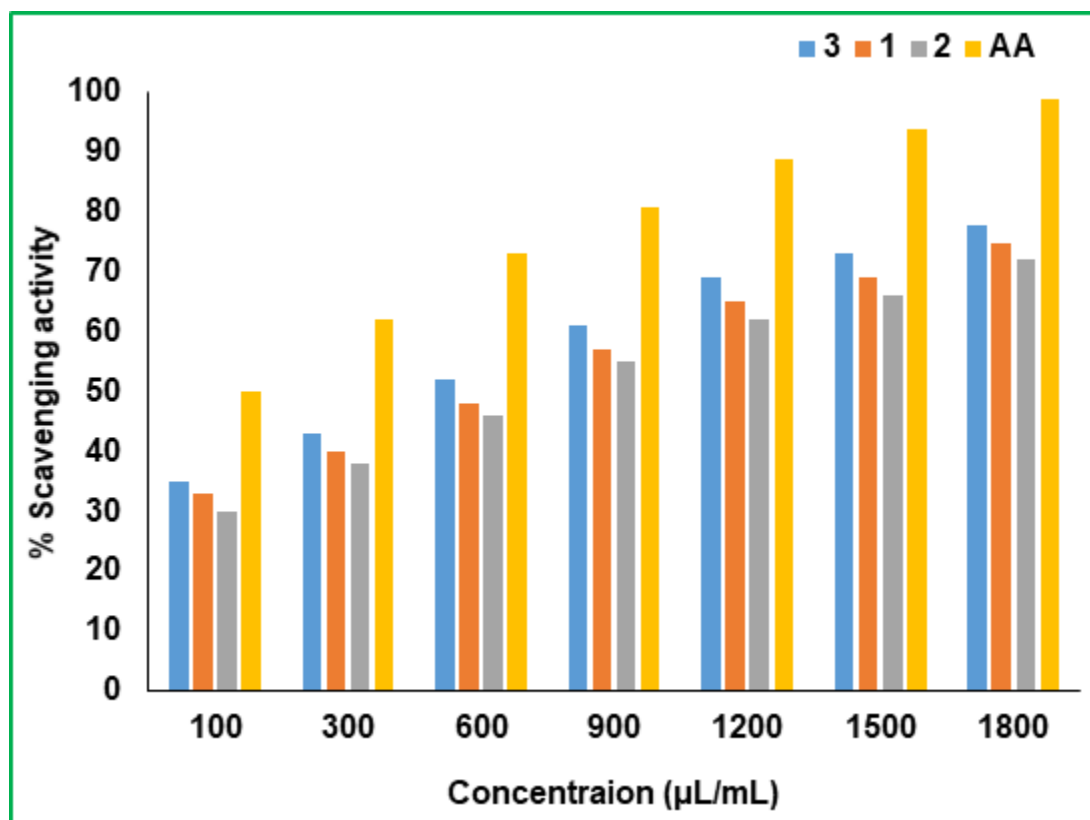


Fig. 8. Viscosity plot for the interaction of 1-3 with DNA.

### 3.7 Antioxidant activity

DPPH is the most widely used radical to determine the reducing or antioxidant potential of a compound. The antioxidant potential of the compounds 1-3 was evaluated from their interaction with DPPH. Compounds having antioxidant potential must reduce the free 1,1-diphenyl-2-picrylhydrazyl (DPPH) radical into 1,1-diphenyl-2-picrylhydrazine by giving an electron to DPPH radical. The DPPH radical has a strong absorption peak at 517 nm with a deep violet color. Upon the addition of various concentration of the compound, the radical nature of the DPPH changes as its unpaired electron gets paired and as a result the decrease in absorbance as well as decolorization occurs [28, 29]. The effect of the various concentration of compounds 1-3 as well as that of ascorbic acid (AA) used as a standard is shown in Figure 9. The activity of all the three isomeric compounds is almost similar and the maximum activity of compounds 1-3 at 1800  $\mu\text{L}/\text{mL}$  concentration are 72, 75, 78%, respectively. The activity of the ascorbic acid at 1800  $\mu\text{L}/\text{mL}$  concentration is 99%.

However, the activity of the compounds 1-3 is lower as compared to ascorbic acid but they possess the antioxidant potential.



**Fig. 9.** DPPH scavenging activity of 1-3 using AA (ascorbic acid) as standard.

### 3.8 Physicochemical properties and ADME parameters

The physicochemical properties, ADME parameters and the violations of drug-likeness rules of the synthesized compounds 1-3 were listed in Tables 7 and 8. The evaluated physicochemical properties are: the molecular weight, topological polar surface area (tPSA), Molar Refractivity, fraction of  $sp^3$  carbon atoms ( $F_{sp^3}$ ) and some Hydrogen Bond properties. tPSA is the sum of surface areas of polar atoms in a molecule and is used to estimate drug transport properties. Low tPSA values in molecules correspond to a higher propensity for transport and tPSA values obtained for the three isomeric compounds 1-3 is  $66.40 \text{ \AA}^2$  which is within the range of values recommended by various drug-likeness filters.  $F_{sp^3}$  is a newer parameter [40] used to evaluate drug-likeness properties of molecules and its values for the three isomeric compounds 1-3 is 0.27. Molar Refractivity is the overall polarity of a molecule and is expected to be in the range from 40 to 130. Molar Refractivity value for the three isomeric compounds 1-3 is 64.65.

1  
2  
3  
4 Lipophilicity is a valuable parameter that affects drug activity in the human body. LogP  
5 values are the most widely used measure of lipophilicity and represents an indicator of drugs  
6 permeability to reach the target tissue in the body. The LogP values used by the different drug-  
7 likeness filters (MLogP for Lipinski filter [41], WLogP for Ghose [42] and Egan filters [43],  
8 XLogP for Muegge filter [44]) and their mean values (consensus LogP) were shown in the Table  
9 8. All other LogP values for the compounds 1-3 obeys general standards ( $< 5$ ).

10  
11  
12  
13  
14  
15 ESOL is aqueous solubility parameter of molecules proposed by Delenay [45] and is  
16 considered one of the key physical properties in drug discovery. ESOL values for the compounds  
17 1-3 belongs to soluble class as shown in Table 7.

18  
19  
20  
21 There are a lot of filter approach in the literature that suggest a set of rules to evaluate drug-  
22 likeness profiles of molecules. The filters discussed in this paper and their rules are as follows.

- 23 • Lipinski (Pfizer) filter [41]:  $MW \leq 500$ ;  $MLogP \leq 4.15$ ;  $HBA \leq 10$ ;  $HBD \leq 5$
- 24 • Ghose filter [42]:  $160 \leq MW \leq 480$ ;  $-0.4 \leq WLogP \leq 5.6$ ;  $40 \leq MR \leq 130$ ;  $20 \leq atoms \leq 70$
- 25 • Veber (GSK) filter [46]:  $RB \leq 10$ ;  $tPSA \leq 140$
- 26 • Egan (Pharmacia) filter [43]:  $WLogP \leq 5.88$ ;  $tPSA \leq 131.6$
- 27 • Muegge (Bayer) filter [44]:  $200 \leq MW \leq 600$ ,  $-2 \leq XLogP \leq 5$ ;  $tPSA \leq 157$ ;  $HBA \leq 10$ ;  $HBD \leq$   
28  $5$ ;  $RB \leq 15$ ; No. of rings  $\leq 7$ ; No. of carbons  $> 4$ ; No. of heteroatoms  $> 1$

29  
30  
31  
32  
33  
34  
35  
36  
37  
38  
39  
40 The filters generally state that an orally active drug should not violate the above criteria  
41 more than once. According to Table 8, it is observed that the compounds **1-3** obey all the filters  
42 and has zero violation.

43  
44  
45  
46  
47  
48  
49 Bioavailability score estimate the probability of a compound to have oral bioavailability in  
50 rat or measurable Caco-2 permeability and the bioavailability score value of a compound in the rat  
51 is expected to be  $> 0.1068$ . A poor bioavailability results in lower activity of the molecule and  
52 higher inter-individual variability, and thus causes an unexpected response of a drug [47]. The  
53 bioavailability score value for the three isomeric compounds is 0.85.

54  
55  
56  
57  
58  
59  
60  
61  
62  
63  
64  
65 Log  $K_p$  is skin permeation parameter suggested by Potts *et al.* [48]; high negative Log  $K_p$   
value of the molecule indicates that the molecule has less penetration into the skin. The value of  
Log  $K_p$  value for compounds 1-3 is -7.24 cm/s, -6.55cm/s and -6.92 cm/s, respectively.

In summary, Tables 7 and 8 show the physicochemical properties, lipophilicity and water  
solubility values of the compounds 1-3 used by various drug filters and have zero violation.  
Moreover, the favorable bioavailability scores and the higher skin absorption indicate that these

1  
2  
3  
4 compounds can be potential drug candidates. The three isomeric compounds **1-3** are Non-  
5  
6 mutagenic, non-tumorigenic, non-irritant and have no reproductive effect.  
7

8 The radar image and the BOILED-Egg model of the synthesized compounds are shown in  
9  
10 Figure 10. The obtained radar image identifies substances that can be considered drug-like in the  
11 pink area through 6 different physicochemical parameters. These parameters are defined as  
12 lipophilicity (LIPO), molecular size (SIZE), polarity (POLAR), solubility (INSOLU), flexibility  
13 (FLEX) and saturation (INSATU). The radar image of the three isomeric compounds completely  
14 falls in the pink area in accordance with 5 different parameters. In the BOILED-Egg model, the  
15 yellow area represents the crossing of the blood-brain barrier, and the white area represents  
16 absorption in the gastrointestinal system. This model is a distribution graph of commercial drugs  
17 by defining the X-axis as the TPSA value of the molecule and the WLOGP value of the Y-axis.  
18 The red dot represents the molecule selected, and inferences about pharmacokinetic properties are  
19 made according to the status of this point in the yellow, white and grey area. As seen in Figure 5,  
20 it was predicted that the compounds 1-3 can be a candidate for such drug molecules with its  
21 absorption status in the blood-brain barrier. On the other hand, there are many factors affecting the  
22 passage of a drug candidate molecule into the lymph and blood circulation. Some of these factors  
23 are the size of the molecule, molecular weight, hydrophilic and lipophilic structure.  
24  
25  
26  
27  
28  
29  
30  
31  
32  
33  
34  
35  
36  
37  
38  
39  
40  
41  
42  
43  
44  
45  
46  
47  
48  
49  
50  
51  
52  
53  
54  
55  
56  
57  
58  
59  
60  
61  
62  
63  
64  
65

**Table 7**Physicochemical properties, lipophilicity, and solubility for **1-3**

Property	1	2	3
<b>Physicochemical Properties</b>			
M. Weight (g/mol)	286.12	286.12	286.12
Fraction Csp <sup>3</sup>	0.27	0.27	0.27
No. rotatable bonds	6	6	6
No. H-bond acceptors/donor	3/2	3/2	3/2
Molar Refractivity	64.65	64.65	64.65
Total polar surface area (Å <sup>2</sup> )	66.40	66.40	66.40
<b>Lipophilicity</b>			
Log <i>P</i> <sub>o/w</sub> (iLOGP)	1.83	1.84	1.73
Log <i>P</i> <sub>o/w</sub> (XLOGP)	1.13	2.10	1.58
Log <i>P</i> <sub>o/w</sub> (WLOGP)	2.45	2.45	2.45
Log <i>P</i> <sub>o/w</sub> (MLOGP)	2.12	2.12	2.12
Log <i>P</i> <sub>o/w</sub> (SILICOS-IT)	2.09	2.09	2.09
Consensus Log <i>P</i> <sub>o/w</sub>	1.92	2.12	2.00
<b>Water Solubility</b>			
Log <i>S</i> (ESOL)	-2.21	-2.82	-2.49
Solubility (mg/mL), Class	1.77, Soluble	4.35e-01, Soluble	9.24e-01, Soluble
Log <i>S</i> (Ali)	-2.12	-3.12	-2.59
Solubility (mg/mL), Class	2.18, Soluble	2.15e-01, Soluble	7.44e-01, Soluble
Log <i>S</i> (SILICOS-IT)	-3.83	-3.83	-3.83
Solubility (mg/mL), Class	4.20e-02, Soluble	4.20e-02, Soluble	4.20e-02, Soluble

**Table 8**

Druglikeness, pharmacokinetics, medicinal chemistry and toxicity risks of 1-3

<b>Property</b>	<b>1</b>	<b>2</b>	<b>3</b>
<b>Druglikeness</b>			
Lipinski	Yes; 0 violation	Yes; 0 violation	Yes; 0 violation
Ghose	Yes	Yes	Yes
Veber	Yes	Yes	Yes
Egan	Yes	Yes	Yes
Muegge	Yes	Yes	Yes
Bioavailability Score	0.85	0.85	0.85
Drug Score	0.44	0.44	0.26
<b>Pharmacokinetics</b>			
Gastrointestinal absorption	High	High	High
BBB permeant	Yes	Yes	Yes
P-glycoprotein substrate	No	No	No
Cytochrome P450 1A2 inhibitor	No	Yes	No
Cytochrome P450 2C19 inhibitor	No	No	No
Cytochrome P450 2C9 inhibitor	No	No	No
Cytochrome P450 2D6 inhibitor	No	No	No
Cytochrome P450 3A4 inhibitor	No	No	No
Log K <sub>p</sub> (skin permeation)	-7.24 cm/s	-6.55 cm/s	-6.92 cm/s
<b>Medicinal Chemistry</b>			
PAINS	0 alert	0 alert	0 alert
Brenk	0 alert	0 alert	0 alert
Leadlikeness	Yes	Yes	Yes
Synthetic accessibility	1.55	1.78	1.49
<b>Toxicity Risks</b>			
Mutagenic	Not	Not	Not
Tumorigenic	Not	Not	Not
Irritant	Not	Not	Not

Reproductive effect

Not

Not

Not

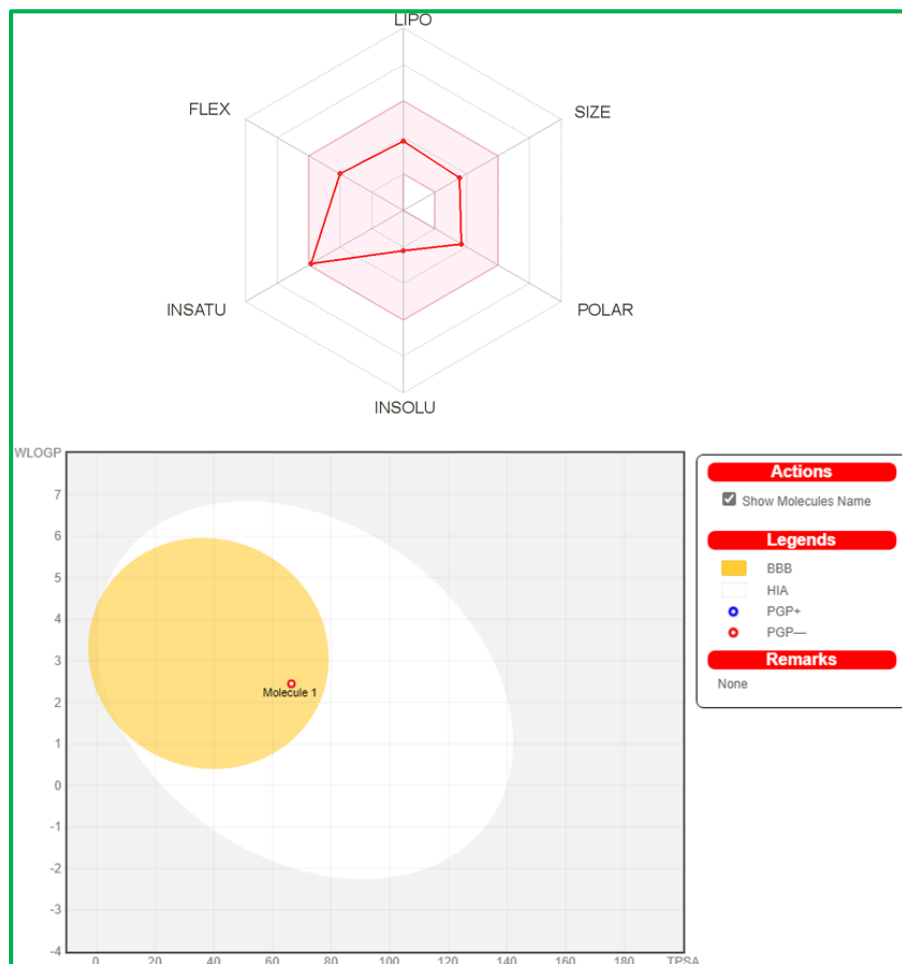


**Fig. 10.** Radar image and the BOILED-Egg model of 1-3.

## Conclusions

Three isomeric carboxylic acid derivatives obtained from the reaction of glutaric anhydride with *ortho*, *meta* and *para* bromoaniline at room temperature just in 2-3 min reaction time. The formation of supramolecular packing structures as a result of intermolecular H-bonding of carboxylic O–H...O and amide–N–H ...O(amide) is the most important characteristics of these compounds. An intercalative binding mode was assigned for the interaction of these compounds with DNA as confirmed by UV-Visible spectroscopic and viscometric methods. The antimicrobial activity of the synthesized compounds performed against 5 bacterial and 2 fungal strains fall in the category of inactive compounds as their inhibition is less than 50%. A maximum of 78% DPPH



1  
2  
3  
4 scavenging at 1800  $\mu\text{L}/\text{mL}$  concentration was shown by the compound-3. The compounds possess  
5  
6 high gastrointestinal absorption and blood brain barrier (BBB) permeant properties. Similarly good  
7  
8 bioavailability scores (0.85), drug score (0.44) and the higher skin absorption indicate that these  
9  
10 compounds can be potential drug candidates.

### 11 12 13 **Acknowledgement**

14  
15 M. Sirajuddin and B. Hanifa are thankful the Higher Education Commission (HEC) Pakistan for  
16  
17 financial support under the NRP Grant # 6796/KPK/NRP/R&D/HEC/2016. The antimicrobial  
18  
19 screening performed by CO-ADD (The Community for Antimicrobial Drug Discovery) was  
20  
21 funded by the Wellcome Trust (UK) and The University of Queensland (Australia). The authors  
22  
23 also gratefully acknowledge Sunway University Sdn Bhd (Grant no. GRTIN-IRG-01-2021) for  
24  
25 support of crystallographic studies.  
26  
27  
28  
29  
30  
31  
32  
33  
34  
35  
36  
37  
38  
39  
40  
41  
42  
43  
44  
45  
46  
47  
48  
49  
50  
51  
52  
53  
54  
55  
56  
57  
58  
59  
60  
61  
62  
63  
64  
65

## References

- [1] M. Sirajuddin, S. Ali, A. Shahnawaz, F. Perveen, S. Andleeb, S. Ali, *J. Mol. Struct.*, 1207 (2020) 127809.
- [2] P. J. Hajduk, M. Bures, J. Praestgaard, S. W. Fesik, *J. Med. Chem.*, 43 (2000) 3443-3447.
- [3] H. Bundgaard, N.M. Nielsen, Prodrug derivatives of carboxylic acid drugs, U.S. Patent 5 (1991) 641, 073.
- [4] H. Pajouhesh, G. R. Lenz, *NeuroRx*, 2 (2005) 541-553.
- [5] C. Ballatore, D.M. Huryn, A.B. Smith, *ChemMedChem.*, 8 (2013) 385-395.
- [6] O Ivasenko, D. F. Perepichka, *Chem. Soc. Rev.* 40 (2011) 191-206.
- [7] P. Tundo, M. Musolino, F. Aricò, *Green Chem.* 20, 28 (2018)
- [8] M. Tahir, M. Sirajuddin, M. Zubair, A. Haider, A. Nadman, S. Ali, F. Perveen, H.B. Tanveer, M.N. Tahir, *J. Iran. Chem. Soc.*, (2021) 1-14.
- [9] C.G. Skinner, D.R. Sargent, *J. Agr. Food Chem.*, 21 (1973) 1057-1060.
- [10] L.H. Hurley, *Nat. Rev. Canc.* 2 (2002) 188-200.
- [11] S.K. Shukla, V.K. Tiwari, R. Sushma, I.C. Tewari, *J. Med. Chem. Lett.* 1 (2011) 10-19.
- [12] CrysAlis PRO, Rigaku Oxford Diffraction, Yarnton, Oxfordshire, England. 2020.
- [13] G. M. Sheldrick, *Acta Crystallogr.*, A71 (2014) 3-8.
- [14] G. M. Sheldrick, *Acta Crystallogr.*, C71 (2014) 3-8.
- [15] L.J. Farrugia, WinGX and ORTEP for Windows: an update, *J. Appl. Crystallogr.* 45 (2012) 849–854.
- [16] DIAMOND, Visual Crystal Structure Information System, Version 3.1, CRYSTAL IMPACT, Postfach 1251, D-530 02 Bonn, Germany, 2006.
- [17] A.L. Spek, CheckCIF validation ALERTS: what they mean and how to respond, *Acta Crystallogr.* E76 (2020) 1–11.
- [18] B. Hanifa, M. Sirajuddin, K.M. Lo, E.R.T. Tiekink, *Z. Kristallogr. - New Cryst. Struct.* 235(6) (2020) 1435–1437.
- [19] B. Hanifa, M. Sirajuddin, H. Khan, K.M. Lo, E.R.T. Tiekink, *Z. Kristallogr. - New Cryst. Struct.* 235(6) (2020) 1481–1483.
- [20] B. Hanifa, M. Sirajuddin, K.M. Lo, E.R.T. Tiekink, *Z. Kristallogr. - New Cryst. Struct.* 235(6) (2020) 1495–1497.
- [21] M. Sirajuddin, B. Hanifa, S. Ullah, H. Khan, K.M. Lo, E.R.T. Tiekink, *Z. Kristallogr. –*

- 1  
2  
3  
4 New Cryst. Struct. 235(6) (2020) 1519–1521.  
5  
6 [22] B. Hanifa, M. Sirajuddin, A. Bari, S.M. Lee, K.M. Lo, E.R.T. Tiekink, Molbank, 2021  
7 (2021) M1209.  
8  
9 [23] B. Hanifa, M. Sirajuddin, Z. Ullah, S. Mahboob, A. Bari, S.M. Lee, K.M. Lo, E.R.T.  
10 Tiekink, Molbank, 2021 (2021) M1227.  
11  
12 [24] a) M. A. T. Blaskovich, J. Zuegg, A. G. Elliott, and M. A. Cooper, ACS Infect. Dis. 2015,  
13 1, 285–287; b) K. A. Hansford, M. A. T. Blaskovich, M. A. Cooper, Fut. Med. Chem.,  
14 2016, 8, 925–929.  
15  
16 [25] B. Iglewicz, D.C. Hoaglin, Volume 16: How to Detect and Handle Outliers. The ASQC  
17 Basic Reference in Quality Control: Statistical Techniques, 1993.  
18  
19 [26] M. Tahir, M. Sirajuddin, A. Haider, S. Ali, A. Nadhman, C. Rizzoli, J. Mol. Struct., 1178  
20 (2019) 29-38.  
21  
22 [27] M. Zubair, M. Sirajuddin, K. Ullah, A. Haider, F. Perveen, I. Hussain, S. Ali, M.N. Tahir,  
23 J. Mol. Struct., 1205 (2020) 127574.  
24  
25 [28] I. Aziz, M. Sirajuddin, A. Munir, S. Tirmizi, S. Nadeem, M.N. Tahir, W. Sajjad, Russ. J.  
26 Gen. Chem., 88 (2018) 551-559.  
27  
28 [29] S. Noureen, M. Sirajuddin, S. Ali, F. Shaheen, M.N. Tahir, Polyhedron, 102 (2015) 750-  
29 758.  
30  
31 [30] A. Munir, M. Sirajuddin, M. Zubair, A. Haider, S.A. Tirmizi, S. Ali, H. Khan, K. Ullah, I.  
32 Aziz, Russ. J. Gen. Chem., 87 (2017) 2380.  
33  
34 [31] M. Sirajuddin, S. Ali, A. Badshah, J. Photochem. Photobio. B: Bio., 124 (2013) 1-19.  
35  
36 [32] M. Sirajuddin, S. Ali, N.A. Shah, M.R. Khan, M.N. Tahir, Spectrochim. Acta Part A Mol.  
37 Biomol. Spectrosc., 94 (2012) 134–142.  
38  
39 [33] M. Sirajuddin, N. Uddin, S. Ali, M.N. Tahir, Spectrochim. Acta Part A Mol. Biomol.  
40 Spectrosc., 116 (2013) 111–121.  
41  
42 [34] A. Daina, O. Michielin, V. Zoete, J. Chem. Inf. Model, 54 (2014) 3284-3301.  
43  
44 [35] A. Daina, O. Michielin, V. Zoete, Sci. Rep., 7 (2017) 42717.  
45  
46 [36] A. Daina, V. Zoete, Chem. Med. Chem., 11 (2016) 1117-1121.  
47  
48 [37] M. Sirajuddin, S. Ali, V. McKee, H. Ullah, Spectrochim. Acta Part A Mol. Biomol.  
49 Spectrosc., 138 (2015) 569–578.  
50  
51 [38] N. Uddin, M. Sirajuddin, N. Uddin, M. Tariq, H. Ullah, S. Ali, S.A. Tirmizi, A.R. Khan,  
52  
53  
54  
55  
56  
57  
58  
59  
60  
61  
62  
63  
64  
65

1  
2  
3  
4  
5  
6  
7  
8  
9  
10  
11  
12  
13  
14  
15  
16  
17  
18  
19  
20  
21  
22  
23  
24  
25  
26  
27  
28  
29  
30  
31  
32  
33  
34  
35  
36  
37  
38  
39  
40  
41  
42  
43  
44  
45  
46  
47  
48  
49  
50  
51  
52  
53  
54  
55  
56  
57  
58  
59  
60  
61  
62  
63  
64  
65

Spectrochim. Acta Part A Mol. Biomol. Spectrosc., 140 (2015) 563–574.

[39] M. Sirajuddin, V. McKee, M. Tariq, S. Ali, Eur. J. Med. Chem., 143 (2018) 1903-1918.

[40] F. Lovering, J. Bikker, C. Humblet, J. Med. Chem., 52 (2009) 6752-6756.

[41] C.A. Lipinski, F. Lombardo, B.W. Dominy, P.J. Feeney, Adv. Drug. Deliv. Rev., 23 (1997) 3-25.

[42] A.K. Ghose, V.N. Viswanadhan, J.J. Wendoloski, J. Comb. Chem., 1 (1999) 55-68.

[43] W.J. Egan, K.M. Merz, J.J. Baldwin, J. Med. Chem., 43 (2000) 3867-3877.

[44] I. Muegge, S.L. Heald, D. Brittelli, J. Med. Chem., 44 (2001) 1841-1846.

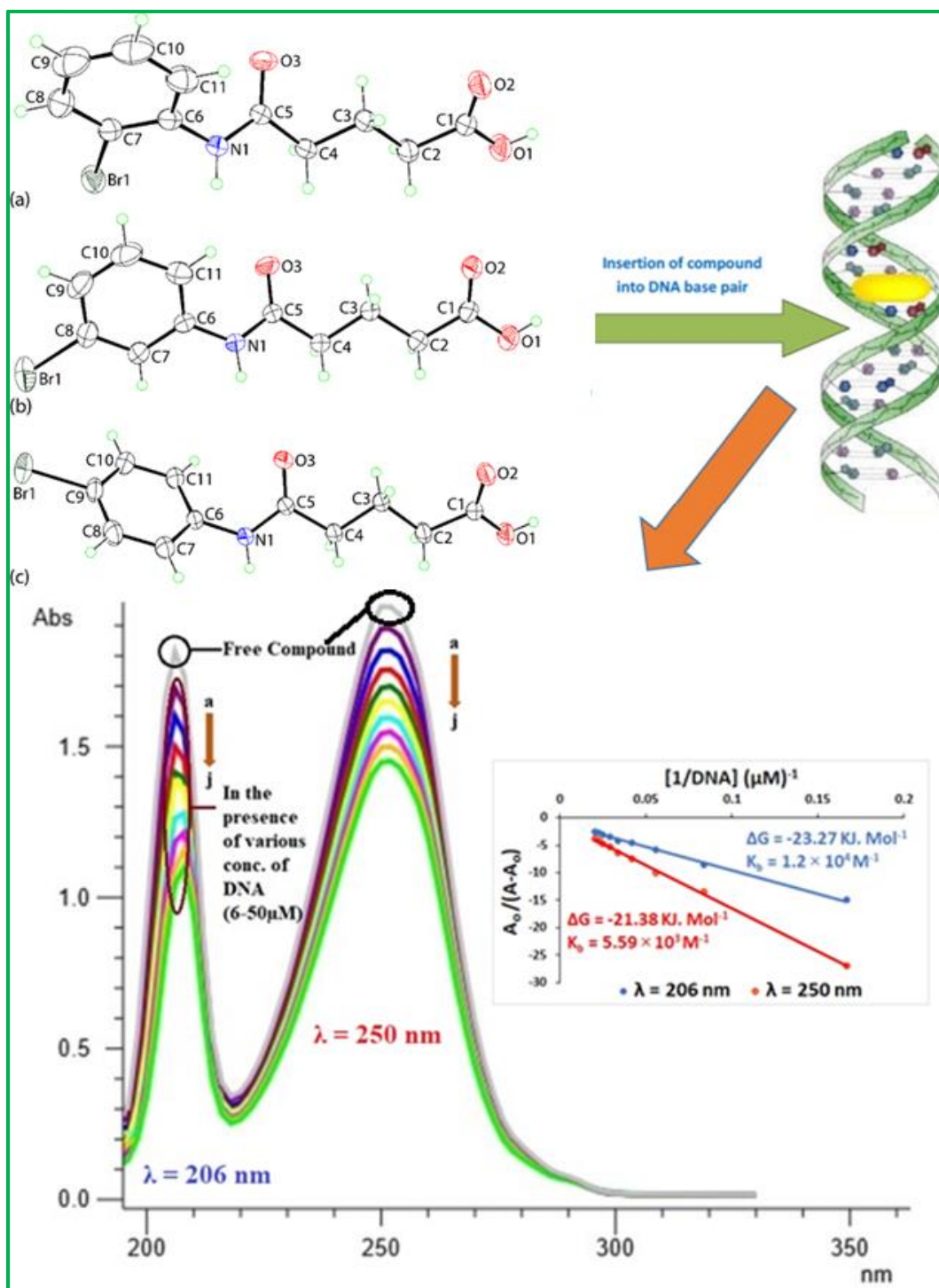
[45] J.S. Delaney, J. Chem. Inf. Model., 44 (2004) 1000-1005.

[46] D.F. Veber, S.R. Johnson, H.Y. Cheng, B.R. Smith, K.W. Ward, K.D. Kopple, J. Med. Chem., 45 (2002) 2615-2623.

[47] Y.C. Martin, J. Med. Chem., 48 (2005) 3164-3170.

[48] R.O. Potts, R.H. Guy, Pharm. Res., 9 (1992) 663-669.

## Graphical Abstract: Pictograph



## Synopsis Graphical Abstract:

The three isomeric carboxylic acid derivatives interact with SS-DNA via intercalative mode which was confirmed by UV/Vis. Spectroscopy and viscometry. They have shown moderate antimicrobial and good antioxidant potentials.



---

The following ALERTS were generated. Each ALERT has the format  
**test-name\_ALERT\_alert-type\_alert-level.**

Click on the hyperlinks for more details of the test.

---

**● Alert level C**

PLAT029_ALERT_3_C	_diffrn_measured_fraction_theta_full	value Low	0.963	Why?
PLAT911_ALERT_3_C	Missing FCF Refl Between Thmin & STh/L=	0.600	79	Report

---

**● Alert level G**

PLAT007_ALERT_5_G	Number of Unrefined Donor-H Atoms	.....	2	Report
PLAT912_ALERT_4_G	Missing # of FCF Reflections Above STh/L=	0.600	94	Note
PLAT913_ALERT_3_G	Missing # of Very Strong Reflections in FCF	....	1	Note
PLAT933_ALERT_2_G	Number of OMIT Records in Embedded .res File	...	8	Note
PLAT941_ALERT_3_G	Average HKL Measurement Multiplicity	.....	1.8	Low
PLAT978_ALERT_2_G	Number C-C Bonds with Positive Residual Density.		1	Info

---

- 0 **ALERT level A** = Most likely a serious problem - resolve or explain
- 0 **ALERT level B** = A potentially serious problem, consider carefully
- 2 **ALERT level C** = Check. Ensure it is not caused by an omission or oversight
- 6 **ALERT level G** = General information/check it is not something unexpected

- 0 ALERT type 1 CIF construction/syntax error, inconsistent or missing data
  - 2 ALERT type 2 Indicator that the structure model may be wrong or deficient
  - 4 ALERT type 3 Indicator that the structure quality may be low
  - 1 ALERT type 4 Improvement, methodology, query or suggestion
  - 1 ALERT type 5 Informative message, check
- 
-

It is advisable to attempt to resolve as many as possible of the alerts in all categories. Often the minor alerts point to easily fixed oversights, errors and omissions in your CIF or refinement strategy, so attention to these fine details can be worthwhile. In order to resolve some of the more serious problems it may be necessary to carry out additional measurements or structure refinements. However, the purpose of your study may justify the reported deviations and the more serious of these should normally be commented upon in the discussion or experimental section of a paper or in the "special\_details" fields of the CIF. checkCIF was carefully designed to identify outliers and unusual parameters, but every test has its limitations and alerts that are not important in a particular case may appear. Conversely, the absence of alerts does not guarantee there are no aspects of the results needing attention. It is up to the individual to critically assess their own results and, if necessary, seek expert advice.

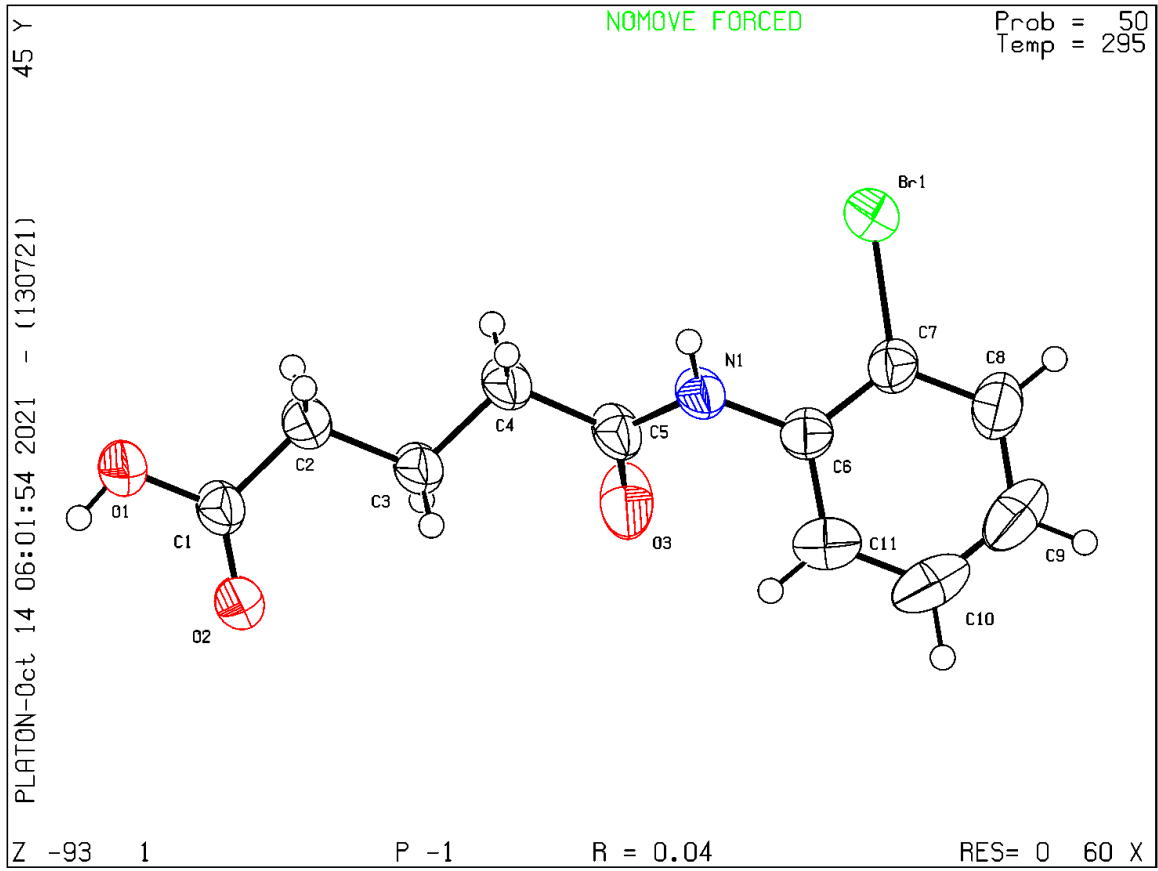
### **Publication of your CIF in IUCr journals**

A basic structural check has been run on your CIF. These basic checks will be run on all CIFs submitted for publication in IUCr journals (*Acta Crystallographica*, *Journal of Applied Crystallography*, *Journal of Synchrotron Radiation*); however, if you intend to submit to *Acta Crystallographica Section C* or *E* or *IUCrData*, you should make sure that full publication checks are run on the final version of your CIF prior to submission.

### **Publication of your CIF in other journals**

Please refer to the *Notes for Authors* of the relevant journal for any special instructions relating to CIF submission.





## checkCIF/PLATON report

Structure factors have been supplied for datablock(s) shelx

THIS REPORT IS FOR GUIDANCE ONLY. IF USED AS PART OF A REVIEW PROCEDURE FOR PUBLICATION, IT SHOULD NOT REPLACE THE EXPERTISE OF AN EXPERIENCED CRYSTALLOGRAPHIC REFEREE.

No syntax errors found.      CIF dictionary      Interpreting this report

### Datablock: shelx

---

Bond precision:      C-C = 0.0046 A

Wavelength=1.54184

Cell:                      a=4.9260 (2)                      b=8.3664 (5)                      c=14.6791 (6)  
                                    alpha=98.247 (4)                      beta=96.176 (3)                      gamma=99.697 (4)  
Temperature:              294 K

	Calculated	Reported
Volume	584.75 (5)	584.75 (5)
Space group	P -1	P -1
Hall group	-P 1	-P 1
Moiety formula	C11 H12 Br N O3	C11 H12 Br N O3
Sum formula	C11 H12 Br N O3	C11 H12 Br N O3
Mr	286.12	286.13
Dx, g cm <sup>-3</sup>	1.625	1.625
Z	2	2
Mu (mm <sup>-1</sup> )	4.748	4.748
F000	288.0	288.0
F000'	287.37	
h, k, lmax	5, 9, 17	5, 9, 17
Nref	2079	2078
Tmin, Tmax	0.597, 0.717	0.790, 1.000
Tmin'	0.541	

Correction method= # Reported T Limits: Tmin=0.790 Tmax=1.000  
AbsCorr = GAUSSIAN

Data completeness= 1.000

Theta (max)= 67.078

R(reflections)= 0.0413 ( 1918)

wR2(reflections)=  
0.1100 ( 2078)

S = 1.062

Npar= 151

---

The following ALERTS were generated. Each ALERT has the format  
**test-name\_ALERT\_alert-type\_alert-level.**

Click on the hyperlinks for more details of the test.

---

 **Alert level C**

PLAT242\_ALERT\_2\_C Low 'MainMol' Ueq as Compared to Neighbors of C1 Check

---

 **Alert level G**

PLAT002_ALERT_2_G	Number of Distance or Angle Restraints on AtSite	4	Note
PLAT172_ALERT_4_G	The CIF-Embedded .res File Contains DFIX Records	2	Report
PLAT860_ALERT_3_G	Number of Least-Squares Restraints .....	2	Note
PLAT909_ALERT_3_G	Percentage of I>2sig(I) Data at Theta(Max) Still	76%	Note
PLAT910_ALERT_3_G	Missing # of FCF Reflection(s) Below Theta(Min).	1	Note
PLAT933_ALERT_2_G	Number of OMIT Records in Embedded .res File ...	1	Note
PLAT978_ALERT_2_G	Number C-C Bonds with Positive Residual Density.	6	Info

---

- 0 **ALERT level A** = Most likely a serious problem - resolve or explain  
0 **ALERT level B** = A potentially serious problem, consider carefully  
1 **ALERT level C** = Check. Ensure it is not caused by an omission or oversight  
7 **ALERT level G** = General information/check it is not something unexpected

- 0 ALERT type 1 CIF construction/syntax error, inconsistent or missing data  
4 ALERT type 2 Indicator that the structure model may be wrong or deficient  
3 ALERT type 3 Indicator that the structure quality may be low  
1 ALERT type 4 Improvement, methodology, query or suggestion  
0 ALERT type 5 Informative message, check
- 
-

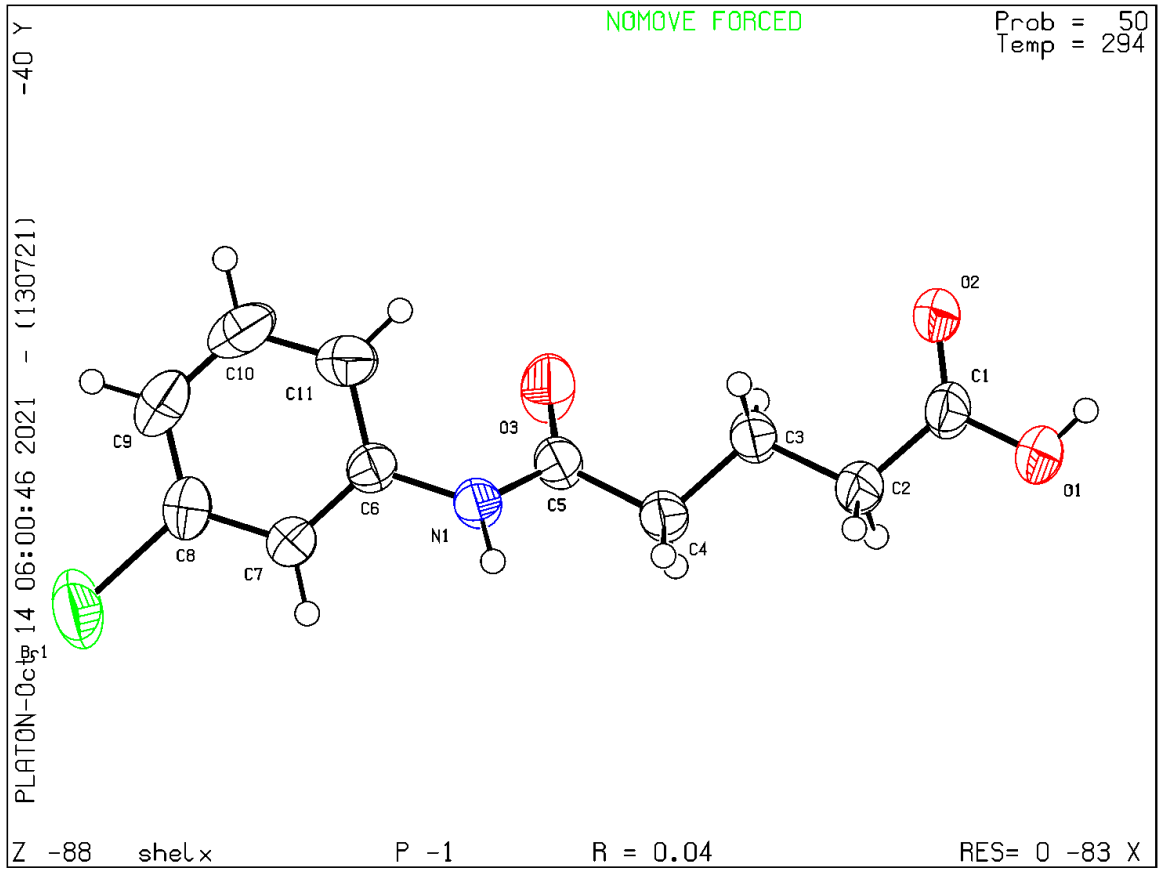
It is advisable to attempt to resolve as many as possible of the alerts in all categories. Often the minor alerts point to easily fixed oversights, errors and omissions in your CIF or refinement strategy, so attention to these fine details can be worthwhile. In order to resolve some of the more serious problems it may be necessary to carry out additional measurements or structure refinements. However, the purpose of your study may justify the reported deviations and the more serious of these should normally be commented upon in the discussion or experimental section of a paper or in the "special\_details" fields of the CIF. checkCIF was carefully designed to identify outliers and unusual parameters, but every test has its limitations and alerts that are not important in a particular case may appear. Conversely, the absence of alerts does not guarantee there are no aspects of the results needing attention. It is up to the individual to critically assess their own results and, if necessary, seek expert advice.

### **Publication of your CIF in IUCr journals**

A basic structural check has been run on your CIF. These basic checks will be run on all CIFs submitted for publication in IUCr journals (*Acta Crystallographica*, *Journal of Applied Crystallography*, *Journal of Synchrotron Radiation*); however, if you intend to submit to *Acta Crystallographica Section C* or *E* or *IUCrData*, you should make sure that full publication checks are run on the final version of your CIF prior to submission.

### **Publication of your CIF in other journals**

Please refer to the *Notes for Authors* of the relevant journal for any special instructions relating to CIF submission.



## checkCIF/PLATON report

Structure factors have been supplied for datablock(s) 2

THIS REPORT IS FOR GUIDANCE ONLY. IF USED AS PART OF A REVIEW PROCEDURE FOR PUBLICATION, IT SHOULD NOT REPLACE THE EXPERTISE OF AN EXPERIENCED CRYSTALLOGRAPHIC REFEREE.

No syntax errors found.      CIF dictionary      Interpreting this report

### Datablock: 2

---

Bond precision:	C-C = 0.0030 Å	Wavelength=1.54184	
Cell:	a=24.6256 (2)	b=4.80980 (5)	c=9.79495 (13)
	alpha=90	beta=97.4563 (10)	gamma=90
Temperature:	295 K		
	Calculated	Reported	
Volume	1150.35 (2)	1150.34 (2)	
Space group	P 21/c	P 1 21/c 1	
Hall group	-P 2ybc	-P 2ybc	
Moiety formula	C11 H12 Br N O3	C11 H12 Br N O3	
Sum formula	C11 H12 Br N O3	C11 H12 Br N O3	
Mr	286.12	286.13	
Dx, g cm <sup>-3</sup>	1.652	1.652	
Z	4	4	
Mu (mm <sup>-1</sup> )	4.827	4.827	
F000	576.0	576.0	
F000'	574.74		
h, k, lmax	31, 6, 12	31, 6, 12	
Nref	2408	2383	
Tmin, Tmax	0.588, 0.713	0.387, 1.000	
Tmin'	0.285		

Correction method= # Reported T Limits: Tmin=0.387 Tmax=1.000  
AbsCorr = MULTI-SCAN

Data completeness= 0.990      Theta (max)= 76.512

R(reflections)= 0.0329 ( 2289)	wR2(reflections)= 0.0953 ( 2383)
S = 1.056	Npar= 147

---

The following ALERTS were generated. Each ALERT has the format  
**test-name\_ALERT\_alert-type\_alert-level.**

Click on the hyperlinks for more details of the test.

---

**Alert level C**

PLAT250\_ALERT\_2\_C Large U3/U1 Ratio for Average U(i,j) Tensor .... 2.3 Note

---

**Alert level G**

PLAT007\_ALERT\_5\_G Number of Unrefined Donor-H Atoms ..... 2 Report  
PLAT910\_ALERT\_3\_G Missing # of FCF Reflection(s) Below Theta(Min). 1 Note  
PLAT912\_ALERT\_4\_G Missing # of FCF Reflections Above STh/L= 0.600 23 Note  
PLAT913\_ALERT\_3\_G Missing # of Very Strong Reflections in FCF .... 1 Note  
PLAT978\_ALERT\_2\_G Number C-C Bonds with Positive Residual Density. 4 Info

---

0 **ALERT level A** = Most likely a serious problem - resolve or explain  
0 **ALERT level B** = A potentially serious problem, consider carefully  
1 **ALERT level C** = Check. Ensure it is not caused by an omission or oversight  
5 **ALERT level G** = General information/check it is not something unexpected

0 ALERT type 1 CIF construction/syntax error, inconsistent or missing data  
2 ALERT type 2 Indicator that the structure model may be wrong or deficient  
2 ALERT type 3 Indicator that the structure quality may be low  
1 ALERT type 4 Improvement, methodology, query or suggestion  
1 ALERT type 5 Informative message, check

---

---

It is advisable to attempt to resolve as many as possible of the alerts in all categories. Often the minor alerts point to easily fixed oversights, errors and omissions in your CIF or refinement strategy, so attention to these fine details can be worthwhile. In order to resolve some of the more serious problems it may be necessary to carry out additional measurements or structure refinements. However, the purpose of your study may justify the reported deviations and the more serious of these should normally be commented upon in the discussion or experimental section of a paper or in the "special\_details" fields of the CIF. checkCIF was carefully designed to identify outliers and unusual parameters, but every test has its limitations and alerts that are not important in a particular case may appear. Conversely, the absence of alerts does not guarantee there are no aspects of the results needing attention. It is up to the individual to critically assess their own results and, if necessary, seek expert advice.

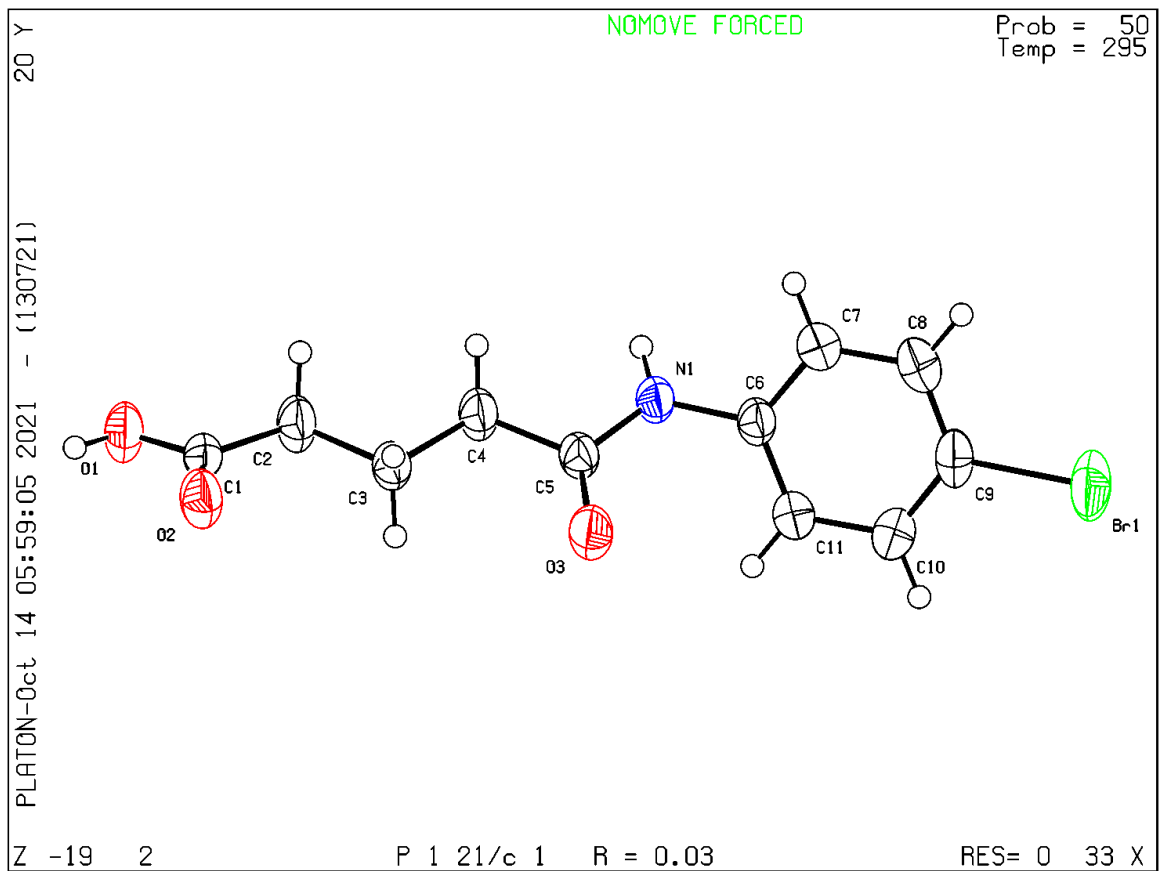
### **Publication of your CIF in IUCr journals**

A basic structural check has been run on your CIF. These basic checks will be run on all CIFs submitted for publication in IUCr journals (*Acta Crystallographica*, *Journal of Applied Crystallography*, *Journal of Synchrotron Radiation*); however, if you intend to submit to *Acta Crystallographica Section C* or *E* or *IUCrData*, you should make sure that full publication checks are run on the final version of your CIF prior to submission.

### **Publication of your CIF in other journals**

Please refer to the *Notes for Authors* of the relevant journal for any special instructions relating to CIF submission.





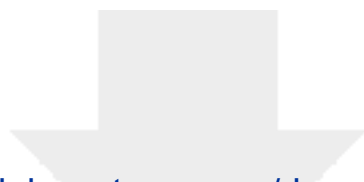


Click here to access/download

**Mol Files**

1.cif

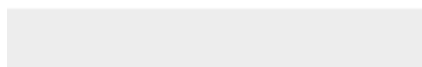
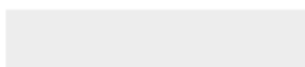


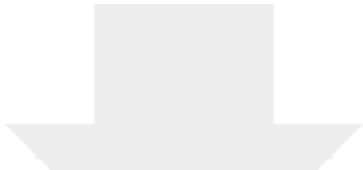


Click here to access/download

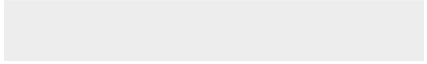
**Mol Files**

2.cif





Click here to access/download  
**Mol Files**  
3.cif



**Declaration of Interest Statement**

The authors declare no conflict of interest.